NTNU

Norwegian University of
Science and Technology

Energy-efficient Supermarket CO2 Compressor Pack with Ejectors

Yi Han

Sustainable Energy
Submission date: February 2017
Supervisor: Trygve Magne Eikevik, EPT
Co-supervisor: Armin Hafner, EPT

Norwegian University of Science and Technology
Department of Energy and Process Engineering

EPT-M-2016-50

MASTER THESIS

for

Student Yi Han
2016

Energy-efficient Supermarket CO₂ Compressor Pack with Ejectors
Energieffektive kompressoranlegg med ejektor i supermarkeder

Background and objective

There is a large transition in supermarket refrigeration with a strong focus on energy consumption. High efficient system configurations with R744 are introduced in various locations throughout Europe; however, further improvements are necessary and possible, for example with the use of ejector-based expansion work recovery.

A multi-ejector expansion module, intended as a substitute for a standard high-pressure electronic expansion valve (HPV) was designed by SINTEF/Danfoss and experimentally investigated at the supermarket compressor rack. Nevertheless, its proper implementation in the compressor rack requires a comprehensive integration with the battery of Medium-Temperature (MT) compressors, Low-Temperature (LT) compressors, and parallel (PAR) compressors. Entirely new pack architectures and operation scenarios must be designed and tested.

To reach this aim, a mathematical model of the R744 refrigeration installation for supermarkets, equipped with the multi-ejector expansion work recovery system, should be formulated, based on commercial software for system analyses (e.g. Engineering Equation Solver, Modelica, etc.). Then, based on simplified operation characteristics of all individual components (compressor, ejectors, heat exchangers, pipelines, storage tanks, etc.), numerical simulations aimed at the minimization of the overall energy consumption in the pack should be performed for specific supermarket load profiles and ambient conditions. According to the estimated energy consumption, the optimum pack configuration together with operation strategy should be specified.

The following tasks are to be consider:

1. Literature review of ejector CO_2 refrigeration systems for supermarkets
2. Analysis of operating conditions for a typical CO_2 compressor rack in supermarket installations
3. Preparation of numerical libraries for components of the compressor packs (ejectors, compressors, etc.)
4. Set up of the numerical model of the compressor pack
5. Numerical simulations aimed at optimization of the pack architecture and operation strategy
6. Experimental investigation of CO_2 refrigeration system with ejectors and analysis of measurement results
7. Make a scientific paper with main results from the thesis
8. Make proposal for further work

Within 14 days of receiving the written text on the master thesis, the candidate shall submit a research plan for his project to the department.

When the thesis is evaluated, emphasis is put on processing of the results, and that they are presented in tabular and/or graphic form in a clear manner, and that they are analysed carefully.

The thesis should be formulated as a research report with summary both in English and Chinese, conclusion, literature references, table of contents etc. During the preparation of the text, the candidate should make an effort to produce a well-structured and easily readable report. In order to ease the evaluation of the thesis, it is important that the cross-references are correct. In the making of the report, strong emphasis should be placed on both a thorough discussion of the results and an orderly presentation.

The candidate is requested to initiate and keep close contact with his/her academic supervisor(s) throughout the working period. The candidate must follow the rules and regulations of NTNU as well as passive directions given by the Department of Energy and Process Engineering.

Risk assessment of the candidate's work shall be carried out according to the department's procedures. The risk assessment must be documented and included as part of the final report. Events related to the candidate's work adversely affecting the health, safety or security, must be documented and included as part of the final report. If the documentation on risk assessment represents a large number of pages, the full version is to be submitted electronically to the supervisor and an excerpt is included in the report.

Pursuant to "Regulations concerning the supplementary provisions to the technology study program/Master of Science" at NTNU §20, the Department reserves the permission to utilize all the results and data for teaching and research purposes as well as in future publications.

The final report is to be submitted digitally in DAIM. An executive summary of the thesis including title, student's name, supervisor's name, year, department name, and NTNU's logo and name, shall be submitted to the department as a separate pdf file. Based on an agreement with the supervisor, the final report and other material and documents may be given to the supervisor in digital format.

☒ Work to be done in lab (Water power lab, Fluids engineering lab, Thermal engineering lab)
☐ Field work

Department of Energy and Process Engineering, March 31st 2016

Prof. Armin Hafner
Academic Supervisor
e-mail: armin.hafner@ntnu.no

Preface

This master thesis was submitted to the Department of Energy and Process Engineering at Norwegian University of Science and Technology and the Institute of Refrigeration and Cryogenics at Shanghai Jiao Tong University. The work was carried out from March of 2016 to January of 2017 within the NTNU-SJTU double master program.

My challenge was to carry out both simulation and experimental work to find the optimum operation strategy of a CO_2 supermarket refrigeration system based on MT, LT and PAR compressor packs. This task gets me to use my gathered knowledge during my study in practice. The work on real test rig gave me large portion of experience and abilities to control the CO2 refrigeration system. I have found motivation in the fact that my work can give information about benefits to operate compressor packs with optimum strategy in the commercial refrigeration systems. Thereby, this thesis can promote energy efficient refrigeration technology for the natural, environmentally friendly refrigerant, such as carbon dioxide.

I would like to express my gratitude to all those who helped me during the whole master years, especially during the thesis work.My deepest gratitude goes first and foremost to Professor Wu Jingyi and Professor Armin and Eikevik, my supervisor of SJTU and NTNU, for their patient and warm encouragement and guidance. She has walked me through all the stages of the writing of this thesis. Without her illuminating instruction, this thesis could never be finished well or integrated.

I would like to express my heartfelt gratitude to Professor Armin and Dr. Ángel Álvarez Pardiñas, who guide me all the stages of experimental work. I am also greatly indebted to Dr. Jin Zhequan, who give me a lot of help both in life and study in Trondheim.

<div align="center">

Shanghai, Jan. 6th, 2017

Yi Han

</div>

ABSTRACT

In this thesis, the background of reimplementation of CO_2 and the description of refrigeration cycles with R744 compressor and ejector are introduced at first. The following is a case study performed to set up the R744 compressor pack model and library. Relevant pre-simulations were also conducted as an overview study. The simulation work for COP analysis was conducted on a system with an ejector and MT, PAR and LT compressors. It is performed with the necessary data from compressor load operation calculation and efficiency test, which are integrated separately before the simulation work. The operation strategy for the system with 4 parallel compressors applied and the reference system with only 2 compressors applied are specified. The COP of each side and the energy consumption of the two strategies are then compared at last.

For load calculation, a simple case study and a real case are analyzed respectively to show how to cover different loads of air conditioning and cooling at medium temperature cabinets with 4 compressors and 2 converters. Also indicated are the load gaps, where the capacity of compressors cannot fully meet the demands. The result provides a design logic and strategy of compressor operation for the simulation work.

For the efficiency test, correlations of oil circulation rate, volumetric efficiency, and overall efficiency with different compressor suction and discharge pressure, and revolutions are made from the experiment result for the SINTEF 6-cylinder compressor. The results are compared with the previous tested efficiency value and two commensurate compressor products used in the pre-simulation for the case study. A correlation between efficiency and frequency is also made to modify the overall efficiency of the compressors selected in simulation work.

At last the operation strategy of the original compressor pack model and the reference model are specified. The daily cooling load in an hourly time scale is assumed and power consumption of each side for both strategies are presented. The two strategies are then compared in terms of COP on each side, energy consumption on each side and total energy consumption of the two strategy during a typical day. The reference strategy saves around 13.1% of energy compared to the original strategy. Some limitations of the model are shown in the end.

KEYWORDS: R744, compressor pack, refrigeration system, COP, operation strategy

List of figures

List of tables

List of Symbols and Abbreviations

Greek letters

η	Efficiency	
π	Pressure ratio	
ρ	Density	kg m^{-3}

Roman Letters

a-e	Coefficient	
h	Specific enthalpy	kJ kg^{-1}
$\dot{m}$	Mass flow rate	kg s^{-1}
n	Compressor frequency	Hz
p	Pressure	bar
P	Power input	kW
Q'	Gas cooler load	%
Q	Cooling load	kW
T, t	Temperature	°C
V_H	Swept Volume	m^3
W	Energy consumption	kW

Subscripts

AC	Air conditioning side
amb	Ambient
c	Cooling
CO_2, R744	Carbon Dioxide
comp	Compressor
elect	Electrical
Ejector, ej	Ejector
evap	evaporator
gc	Gas cooler

high	High side pressure level
in	Inlet
intermediate	Intermediate pressure level
is	Isentropic
low	Low side pressure level
LT	Low temperature side
m	Total mass
medium	Medium pressure level
MT	Medium temperature side
mn	Motive nozzle
o	Mass of oil
out	Outlet
PA	Parallel
revised	Modified model
sn	Suction nozzle
theoretical	Theoretical mass flow
total, overall	Overall
vol	Volumetric

Abbreviations

CD	Dorin compressor seires
COP	Coefficient of performance
EXV	Expansion valve
HPV	High-pressure electronic expansion valve
IHX	Internal Heat Exchanger

Content

1 Introduction

The current situation of the ozone layer and greenhouse emission levels has encouraged research on environmentally friendly natural refrigerants such as CO_2 as an alternative to traditional common used in refrigeration, such as Chlorofluorocarbon (CFC) and hydro-chlorofluorocarbons gases (HCFCs). Part of the recent work on CO_2 refrigeration systems has focused on transcritical CO_2 systems using two-phase ejectors. Two-phase ejectors can be used to reduce the inherent throttling losses of the expansion valve in transcritical CO_2 systems.

Ejectors improve the efficiency of transcritical CO2 systems, but they need of a smart implementation to achieve a smooth control of the systems with changing refrigeration loads. An approach in this line is the multiple ejector. Increased energy efficiency is the most efficient, the least expensive, and the least politically controversial path to a sustainable energy future: Energy saved does not cause emissions, and energy not used reduces the need for new controversial power plants and expensive distribution infrastructure.

A multi-ejector expansion module (MULTIJET), intended as a substitute for a standard high-pressure electronic expansion valve (HPV) was designed by SINTEF/Danfoss and experimentally investigated at the supermarket compressor rack. Nevertheless, its proper implementation in the compressor rack requires a comprehensive integration with the battery of Medium-Temperature (MT) compressors, Low-Temperature (LT) compressors, and parallel (PAR) compressors. Entirely new pack architectures and operation scenarios must be designed and tested.

Therefore, this project report is focused on formulating a mathematical model, based on EES, of the R744 refrigeration installation for supermarkets equipped with the multi-ejector expansion work recovery system. Then, based on simplified operation characteristics of all individual components (compressor, ejectors, heat exchangers, pipelines, storage tanks, etc.), numerical simulations aimed at the minimization of the overall energy consumption in the pack will be performed as a function of, for example, supermarket load profiles and ambient conditions. According to the estimated energy consumption, the optimum pack configuration together with operation strategy will be specified.

This report begins with the refrigeration cycles with R744 compressor. A literature review of the published studies about the R744 multiple ejector refrigeration system is given. Simulation work and experimental test are conducted subsequently to build 2 operation strategies. The results, discussion, and conclusions are presented at the end.

2 Review of supermarket refrigeration system

2.1 Historical background and the re-implementation of R744

Implementation of R744 refrigeration system in supermarkets started with the renaissance of R744 as refrigerant. In 1990 Gustav Lorentzen received a patent in which he described a transcritical carbon dioxide vapor compression cycle, initiating a renaissance for R744 as a refrigerant [1] (Elbel, 2007). Regarding the properties of R744 as a refrigerant, Lorenzten pointed out that because of the high working pressures and the large pressure difference between the heat absorption and heat rejection sides, the difference between the isenthalpic throttling and the isentropic expansion gets more pronounced. Robinson and Groll[2] (1998) found that the isenthalpic expansion process in a transcritical R744 refrigeration cycle is responsible for approximately 40% of the cycles' irreversibility. When an isentropic expander with a 60% efficiency is applied, the percentage decreases to around 25%. In order to recover the energy lost during throttling of the fluid, it would be required to change the expansion process from possessing an isenthalpic behavior towards a more isentropic character [3] (Kornhauser, 1990). However, ejector geometric parameters and system configurations have significant impact on system performance, which means the results of certain ejector researches can be explained only in one or two working conditions or configurations as the papers described and are usually not applicable or generalized in others. Thus lots of new researches are increasingly focused on case studies of both numerical and experimental analysis.

According to Elbel[4](2011), Drescher et al. [5] (2007), Banasiak et al.[6] (2012), Fiorenzano[7] (2011) and Lucas and Koehler[8] (2012), R744 ejectors may improve the system efficiency by up to 15%, depending on the ambient temperature of the heat rejection device of the refrigeration system. Different multi stage R-744 supermarket refrigeration systems were also investigated in the past by Gernemann[9] (2003), Kruse and Schiesaro[10] (2002), Froeschle[11] (2009) and Sawalha[12] (2008), but no ejector system in a supermarket application can be found in literature.

2.2 Review of R744 supermarket refrigeration systems

At very beginning, R744 systems for supermarkets were applied without ejectors. Girotto et al.[13] (2004) introduced a typical commercial refrigeration system using R744 as the refrigerant. This was one of the earliest reapplications of R744 in supermarket. The system was installed in a supermarket with a sales area of about 1200 m^2. It has a total cooling capacity of 120 kW at medium temperature (MT-evaporating temperature -10°C) and about 25 kW in low temperature (LT-evaporating temperature -35°C). The system is illustrated in figure 1.
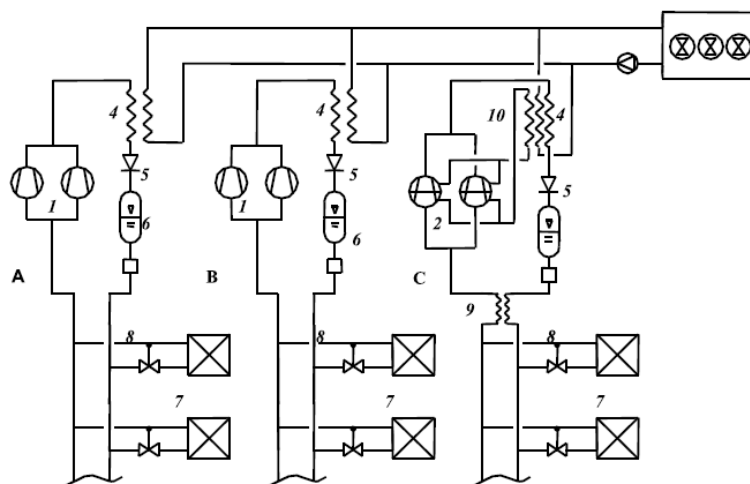
Fig. 1 R744 compressor pack design

The COP and electric power consumption of the compressors of the all-CO₂ system was compared to that of an equivalent R404A plant. The authors observed that when the same kind of calculation is referred to different climates, the all-CO₂ system can have an equivalent or lower energy consumption than the R404A direct expansion system, due to the higher percentage of hours in which external temperature is lower than 10 °C, therefore favorable to CO_2. On the other hand, the limitations of this refrigeration system were given at the end and corresponding further suggestions are given as well that three kinds of facilities should be utilized to increase system efficiency: direct heat rejection to the ambient air with a fin-coil gas cooler, auxiliary cooling with a hybrid cooler, and piping layout with suction of flash gas to second stage from the top of the liquid receiver.

The later researches ameliorated this system by implementing ejectors and other auxiliary facilities. Sharma et al.[14] (2014) presented an analysis of various CO_2 transcritical and cascade/secondary loop refrigeration systems that were becoming popular in supermarket applications with the objective of optimizing the operating parameters of these systems. In addition, the performance of selected CO_2-based refrigeration systems was compared to the baseline R404A multiplex direct expansion system using bin analyses in the eight climate zones of the United States. The Transcritical Booster System with Bypass Compressor (TBS-BC) had the lowest energy consumption for ambient temperatures (T_amb) lower than 8 °C, and for higher ambient temperatures the R404A direct expansion system was found to have the lowest energy consumption. Also, the TBS-BC performs equivalent to or better than the R404A direct expansion system in the northern two-thirds of the US. For the southern portion of the US, the R404A multiplex DX system performs better than CO₂ systems. Specifically, Sharma et al. stated that the COP of the R744 parallel compression system is 13% higher than that of the R404A multiplex (US north) direct expansion system. In the south part of the US, the COP of the parallel compression system is 8.3% lower that of the R404A DX system.

The R744 parallel compression refrigeration systems is a competitive commercial refrigeration system in particular in cold climate regions. Anyway there is still large potential to improve the energy performance of CO_2 systems by reducing the throttling losses. An approach is to introduce multi-ejector as a main expansion device in refrigeration system in order to recover some potential work.

Based on the past research on ejector-based refrigeration systems, the multi-ejector concept was described and theoretically analyzed in a paper by Hafner et al.[15] (2014a). This paper described as well a calculation method to calculate efficiencies and capacities for two different supermarket system layouts. Non-controlled ejectors and additional functions such as heat recovery were evaluated in order to improve the energy efficiency of the system. Results of existing studies show relevant improvements in R774 system efficiency when heat recovery has been adopted. Compared to other refrigerants R744 is particularly suitable for heat recovery applications due to its operation mode close to the critical point.

Among the most important results in Hafner et al. (2014a), the dynamic modelling for supermarket refrigeration and heat recovery systems with multiple ejectors revealed that the multi-ejector system offers a significant increase in the COP for the cooling and heating modes. Measurements carried out with an ejector prototype show that a pressure lift between 2 bar and 6 bar can be reached with an averaged ejector efficiency of about 20%. The multi-ejector system was designed based on cycle simulations The COP increase in three different typical cities were described as comparison that it depends closely on control strategy, specifically 17% in Athens, 16% in Frankfurt and 5% in Trondheim in the summer and the typical COP increase was between 20% and 30%. Hafner and co-workers indicate that the future work should focus on optimizing the control strategy in order to enlarge the energy efficiency for cooling and heat recovery in different climate zones, including installations with intermediate heat storage facility, to avoid peak demand operations.

Wiedenmann et al.[16] (2014) presented an experimental work of a R744 transcritical parallel compression refrigeration system in Migros Bulle supermarket after the integration of the ejectors. Figure 2 shows the schemas of the Migros Bulle refrigeration system with and without the ejectors. The system consists of two vapour and one liquid ejectors. Therefore an additional liquid receiver after the MT evaporator is applied. Wiedenmann et al. stated that the annual energy power consumption, depending on the climate region, of the refrigeration system with integrated ejectors was in the range of 12% to 20% less than the reference system.
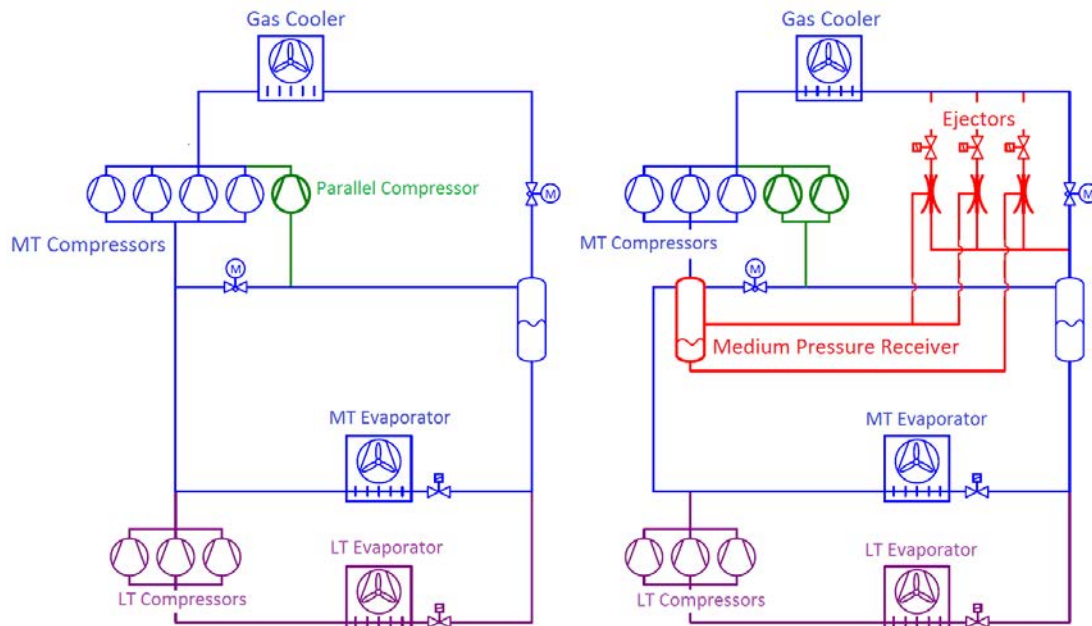
Fig. 2 CO₂ transcritical parallel compression refrigeration systems without (left) and with (right) vapour and liquid ejectors applied in Migros Bulle supermarket.

Recent work on R744 systems has been focused on transcritical R744 systems using two-phase ejectors as the two-phase ejectors can be used to reduce the inherent isenthalpic throttling losses of the expansion valve and increase the system energy efficiency by utilizing the expansion work available when the high side pressure refrigerant is expanded in a motive nozzle inside an ejector. Because it significantly reduces the compressor pressure ratio and the required compression work.

A large number of research work were focused on investigating the energy need for R744 system under different cooling loads and ambient temperatures, which are also presented as configurations of R744 refrigeration systems.

Hafner et al.[17] presented 6 typical refrigeration systems that use R744 as refrigerant: (i) standard booster cycle, (ii) expander cycle, (iii) R744 booster cycle with mechanical sub-cooler units (CO₂ as refrigerant), (iv) economizer 1 cycle with flash tank and parallel compression system, (v) Economizer 2 cycle with parallel compression system and (vi) ejector supported parallel compression system. 4 different levels of cooling loads are chosen as comparison in this numerical study. The pressure drop in the gas coolers, the temperature difference between the outlet temperature of the refrigerant and the inlet temperature of air and the pressure of the flash tank are separately set. Figure 3 illustrates the mechanical sub-cooler system and ejector system.
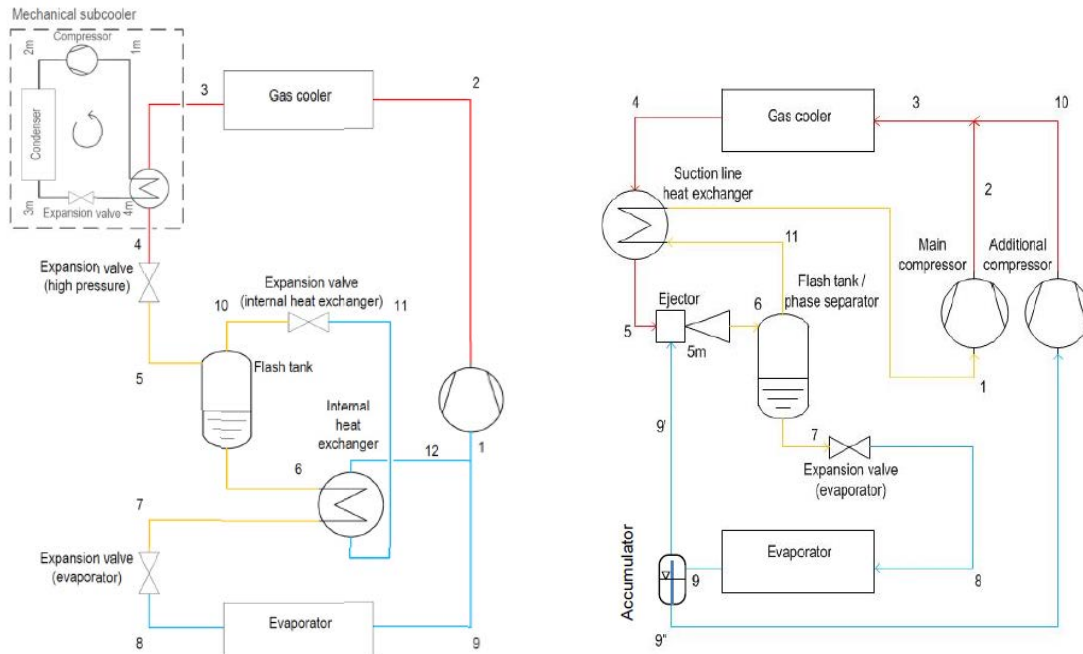
Fig. 3 R744 booster cycle with mechanical sub-cooler and ejector supported parallel compression system

The cooling capacity required for mechanical sub-cooler is presented under different ambient temperatures through two different approaches in order to investigate the working conditions to meet the selected cooling loads. The maximum COP that can be achieved indicated as well, which shows that when the cooling need is relatively large, the mechanical sub-cooling system works with high efficiency. Additionally, the COP of the expander system depends significantly on the cooling load; it decreases as the cooling load rises. Besides the ejector efficiency has little impact on the system efficiency, which can be better used than other systems in high ambient temperature. Nevertheless, due to the immature facilities design and system arrangements, the ejector parallel compression systems are not widely used in supermarkets yet. Instead, the Economizer 1 cycle system and the R744 booster system with mechanical sub-cooler units are being the main stream systems that are applied in the supermarkets.

Specifically in the same work, Hafner et al. conducted a set of case studies on several cities selected all over the world. The temperature range and number of hours were collected and integrated to be used as working conditions of the refrigeration systems. The simulation results were compared with the experimental results of Finckh[18] (2011). Two systems including the mechanical sub-cooling system and ejector supported system were compared, and the standard R744 booster baseline system was also referred to as a reference system. The results show the energy consumption of several selected cities, where the COP and cooling load of the three systems varies with different ambient temperatures. The case with R404A applied is compared in certain cities as references. It is indicated that when the ambient temperature is not over 42 °C, the efficiency of the mechanical sub-cooling system or the ejector supported system would be higher than HFC systems. Figures 4 and 5 respectively show the results of the

efficiency analysis both numerically and experimentally and the energy consumption of the selected commercial refrigeration systems in selected cities. HFC systems were set to 100% to be referred to as reference system consumption for the others. In addition, the same numerical calculation has also been conducted in several Chinese cities by Hafner et al.
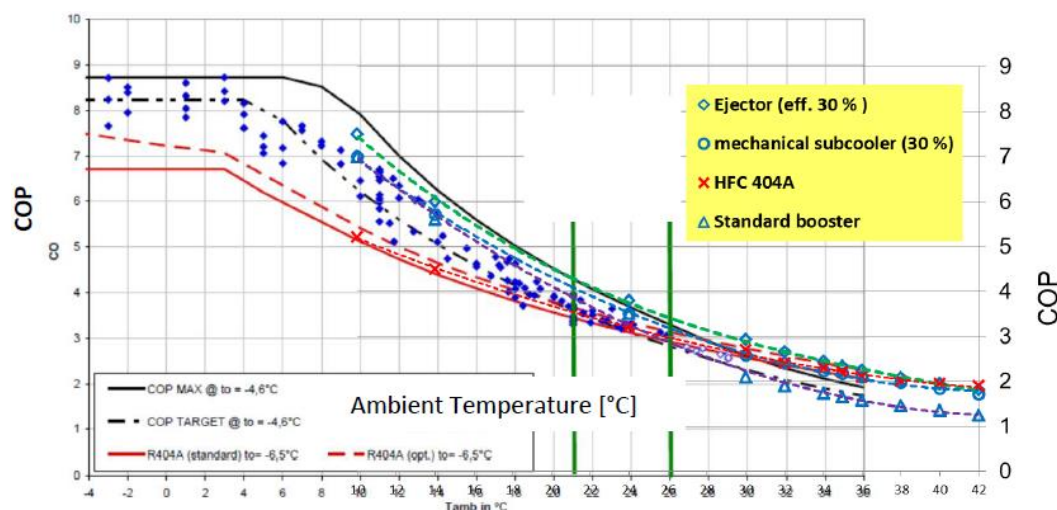
Fig. 4 High ambient conditions of R744 units. HFC performance extrapolated towards 42°C.
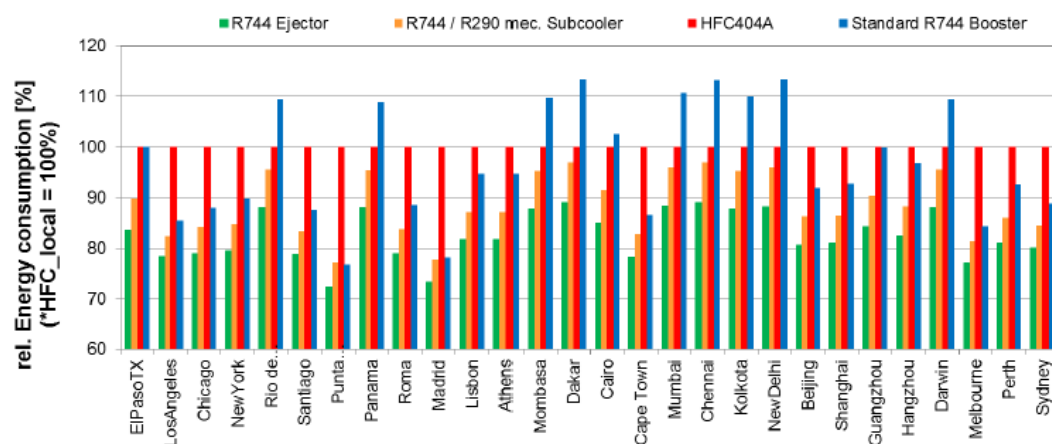
Fig. 5 Relative annual energy consumption of alternative commercial refrigeration systems. Local HFC systems are set to 100%.

Dokandari et al.[19] (2014) evaluated thermodynamically the ejector utilization's impact on the performance of the cascade cycle that uses R744 and R717 as refrigerants. The theoretical analysis shows that the maximum COP and the maximum second law efficiency are on average 7 and 5 percent higher than with the conventional cycle and the exergy destruction rates are roughly 8 percent lower than with the conventional cycle. Therefore, this ejector-expansion cascade cycle is a promising refrigeration cycle. The layout for such a cascade system using R744 and R717 and the corresponding pressure - specific enthalpy diagram are shown in figure 6.
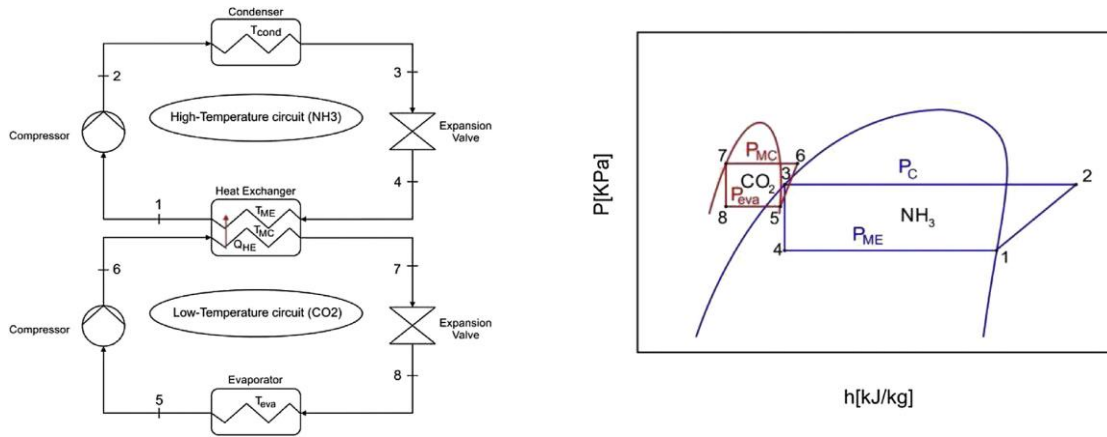
Fig. 6 Expansion cascade cycle using R744 and R717

Lawrence et al.[20] (2014) made a numerical study to compare three refrigeration systems, each of them with three working refrigerants namely R744, propane and ammonia. The schematic cycles of the three system are shown in figure 7.
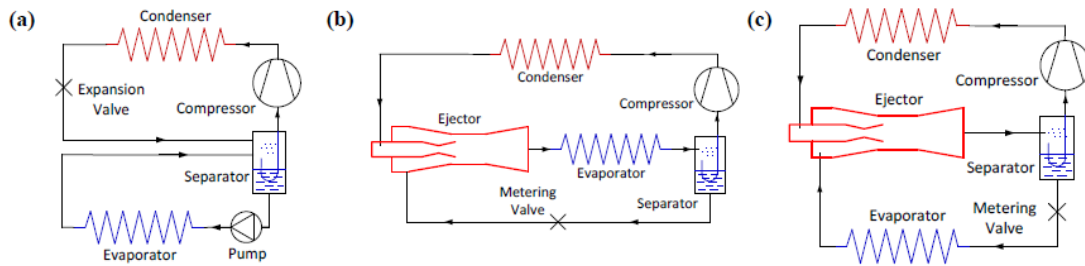
Fig. 7 Cycle layout diagrams of (a) forced recirculation cycle, (b) ejector recirculation cycle, and (c) standard two-phase ejector cycle

The efficiency of every system was presented as COP ratio vs. circulation number and the results were illustrated in figure 8.
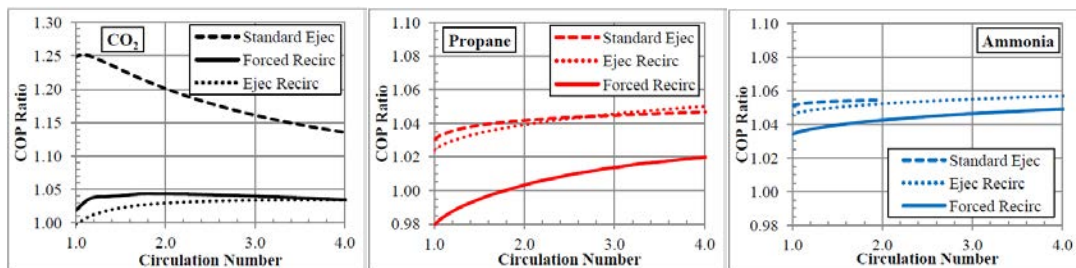
Fig. 8 Performance comparison of the three recirculation cycles as a function of circulation number for CO2, propane, and ammonia

Several conclusions have been reached: a) ammonia is better fitted for forced recirculation system rather than expansion work recovery system, while R744 can be used to achieve higher COP with ejector recovery system; b) both forced recirculation and ejector recirculation systems can only obtain efficiency benefit from liquid recirculation process; c) the standard ejector cycle can be used to increase compressor

suction pressure and provide liquid recirculation simultaneously; d) COP of the ejector recirculation system is irrelevant to the efficiency of the ejector itself because the pressure increase in the ejector is used to overcome pressure drop through evaporator and metering valves.

Lawrence et al. also indicated the effect of ejector geometry on the performance of two-phase R744 ejector in this paper. Three most important parameters, mass entrainment ratio, suction pressure ratio and ejector power recovery efficiency were investigated and several parameters were compared and analyzed, including diffuser geometry, mixing section geometry and motive nozzle geometry. It is showed that geometry has been overlooked for a long period, but actually it is closely related to ejector efficiency. Nevertheless, ejectors with specific geometry parameters can hardly be applied in different systems. Thus the researches focused on geometry of ejectors are not enough to create generalized principles.

Besides the numerical studies aforementioned, the experimental researches conducted in the past few years also contribute to the development of R744 refrigeration systems for supermarket. These papers are mainly focused on the effect of ejector efficiency on the system performance. The energy saving effect of ejectors was experimentally verified by laboratory tests for the single-ejector system. Simulations and experiments showed that compared to conventional system, the COP of the commercial refrigeration systems equipped with a single ejector could be increased 20% at high ambient temperatures. Experimental work performed by Elbel et al.[21] (2011) showed a COP and cooling capacity increase of 7% and 8%, respectively. Elbel introduced a new parameter describing the efficiency of the ejector. According to this new definition, the ejector responsible for the increase in COP operated with an efficiency of 14.5%. Elbel also investigated the effects of internal heat exchange between the compressor suction stream and the gas cooler exit stream. He demonstrated that the internal heat exchanger (IHX) reduced the work recovery potential, as both the ejector and the IHX competed for the same thermodynamic availability. Banasiak et al.[22] (2015) experimentally found a maximum COP improvement over the standard (expansion valve) system of over 8%, This maximum occurred when the ejector was operating at an efficiency of 28.2%. The study focused on optimizing ejector geometries, and individual ejector efficiencies as high as 31% were reported. The authors concluded that in order to investigate the real potential in COP gain, attention should be given to the optimization of the COP for the overall system. Lucas and Koehler[23] (2012) demonstrated experimentally that a COP gain of 17% over the standard cycle is possible with an ejector performing with an efficiency of 22%. In addition, Jie Xiong et al.[24] (2014) conducted a set of comparison experiments to investigate the optimum operating conditions for achieving better performance of a certain R744 heat pump system with one-phase ejector. They aimed to find a correlation between high side temperature or pressure and system efficiency, which includes entrainment ratio, overall COP, actual COP and ejector efficiency. The cycle arrangement of the system is shown in figure 9.
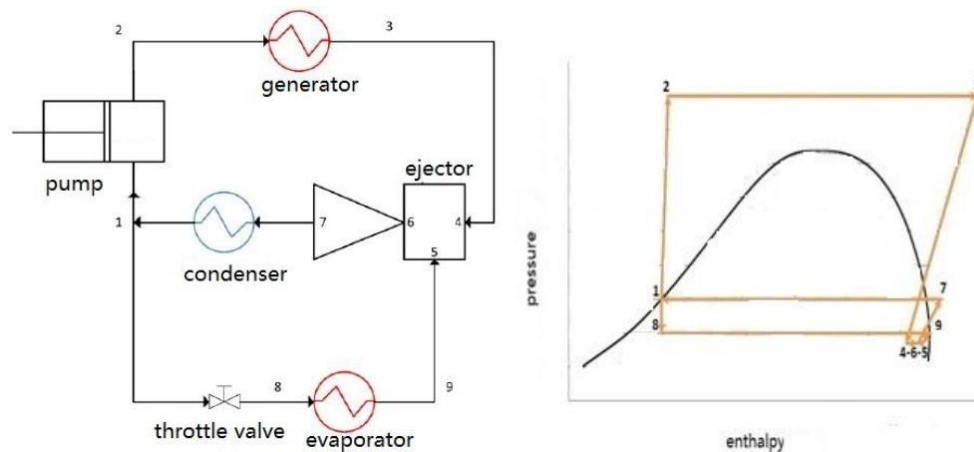
Fig. 9 Schematic representation of the one-phase ejector cycle of expansion work recovery (left) and its pressure-enthalpy diagram (right)

The system working conditions were set to a certain status, with fixed evaporator pressure 51 bar, fixed condensing pressure 58 bar, high side pressure range 70-120 bar and high side temperature 85-100 ℃ . The experiments compared the performance change with high side pressure (and constant high side temperature), and with high side temperature (and constant high side pressure). Results show that with the constant high side temperature, while the ejector efficiency has a peak value at a certain pressure, the entrainment ratio, the overall COP and actual COP go down as the pressure lifts. This means that the overall COP is affected by entrainment ratio and pressure lift is not a benefit for actual COP. The other set of comparison showed that for the constant high side pressure, the ejector efficiency increases as temperature rises, but the other three parameters have peak values. Therefore, the mass entrainment ratio does not affect directly the system performance but is the decisive factor of overall COP. It is also emphasized that the actual COP is the most important efficiency parameter that should be taken into consideration.

2.3 Newest research of R744 compressor pack with ejectors

Gay[25] (1931) was the first person to propose the use of the two-phase ejector for work recovery application in a refrigeration system, so the basic transcritical R744 ejector cycle is based on his idea. The cycle has become the standard cycle for transcritical R744 ejector cycle and been the focus for the majority of the ejector studies. This cycle uses a two-phase ejector as expansion mechanism and has a liquid-vapor separator. The refrigerant flow from the separator is separated into two flows. The vapor is compressed and cooled through the gas cooler, and then enter the motive nozzle of the ejector. The liquid is going to the evaporator to evaporate to vapor, and then enter the suction nozzle of the ejector. The motive stream entrains the suction stream, and both flows mix in the mixing chamber. In the diffuser, the mixed flow undergoes an increase of pressure and in this way, the ejector can improve the performance the cycle.

In addition to the basic R744 ejector cycle described by Elbel, Hafner et al.[17] (2014) presented ejector technology for supermarket applications and carried out analysis of a

simulation model of the multi-ejector system and the reference CO_2 transcritical booster system for the selected load profiles, controls concept and climate data. The transient simulations were performed based on the annual variable ambient temperature and annual variable load profiles for heating and cooling mode, for three different climate regions: North European, Middle European and Mediterranean. In addition, experimental analysis of both foregoing refrigeration systems was presented. To simplify the refrigeration systems, calculations were done for only medium-temperature evaporation level due to the fact that for both systems less than 20% of the overall cooling capacity is provided for the low-temperature cabinets (Hafner et al., 2014).

Figure 10 shows the multi-ejector R-744 system with non-continuously controllable ejectors. The presented system shows the most important part of the supermarket refrigeration system, which maintains the temperature inside the cooling cabinets. Heat from the freezing part of the system is rejected to the medium temperature part. From this part the heat is released to the different heat recovery units and external heat rejection devices (schematically shown as gas cooler GC and inter-stage cooler IC) before the refrigerant enters the expansion devices. In this case the ejectors replace the ordinary expansion valves, which do not recover the expansion work.

The novel R-744 commercial refrigeration system solutions including non-continuously controlled ejectors with different ejector geometries allow applying standardized ejectors. With different cross sections in the motive nozzles the high side pressure can be controlled in accordance to the ambient temperature or load requirements. The MT compressors are sucking from the gas phase of the first separator (SP-1) downstream of the ejectors. The ejectors are applied to maintain a certain pressure difference between the separator (SP-2) and the separator (SP-1). In case of a reduced pressure lift capability of the ejectors, one of the MT compressors (rpm controlled) can be connected to the vapor outlet of the separator (SP-2) and thereby reduce the entrainment ratio.

This supports the ejectors in operation to maintain a certain flow rate of refrigerant via the ejector into the separator, even at low high side pressures. This solution secures a constant pressure difference between both separators.
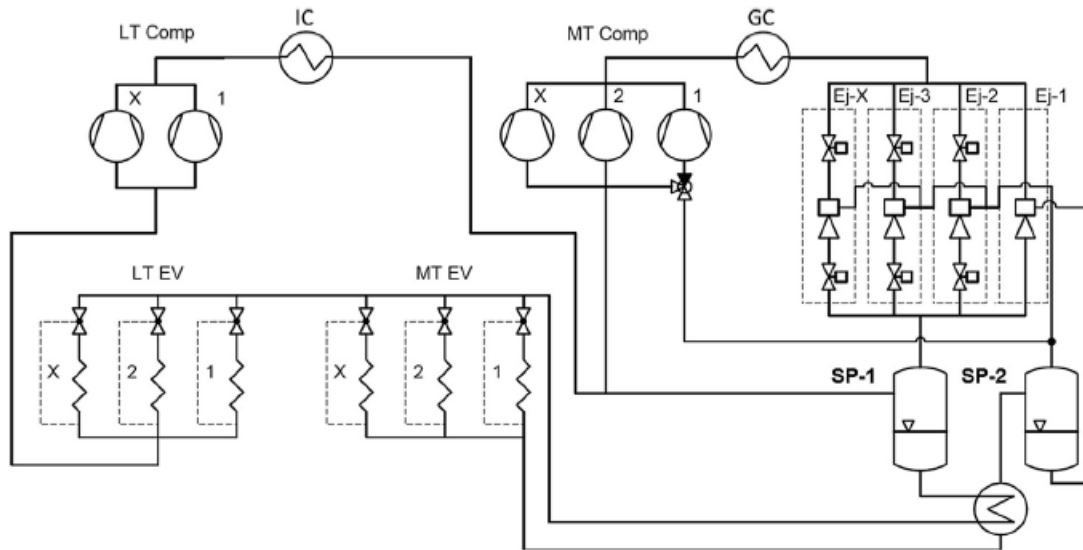
Fig. 10 Circuit diagram of supermarket refrigeration and heating system with multi-ejector R-744 concept with non-continuously controllable ejectors[15]

Banasiak et al. (2015) investigated a multi-ejector expansion pack, intended as a substitute for a standard high-pressure electronic expansion valve (HPV). Four different ejector cartridges were sized to enable a discrete opening characteristic with a binary profile for a parallel-compression R744 system. The system is rated for 70 kW MT cooling load at 35 °C gas cooler outlet temperature and -3 °C evaporation temperature. High values of ejector efficiency, exceeding 0.3 over a broad operation range, were recorded for the four cartridges tested under vapor compression conditions. The applicability of the multi-ejector pack as a main flashing device was verified experimentally. The schematics of the multi-ejector facilities are shown in figure 11.

(a)
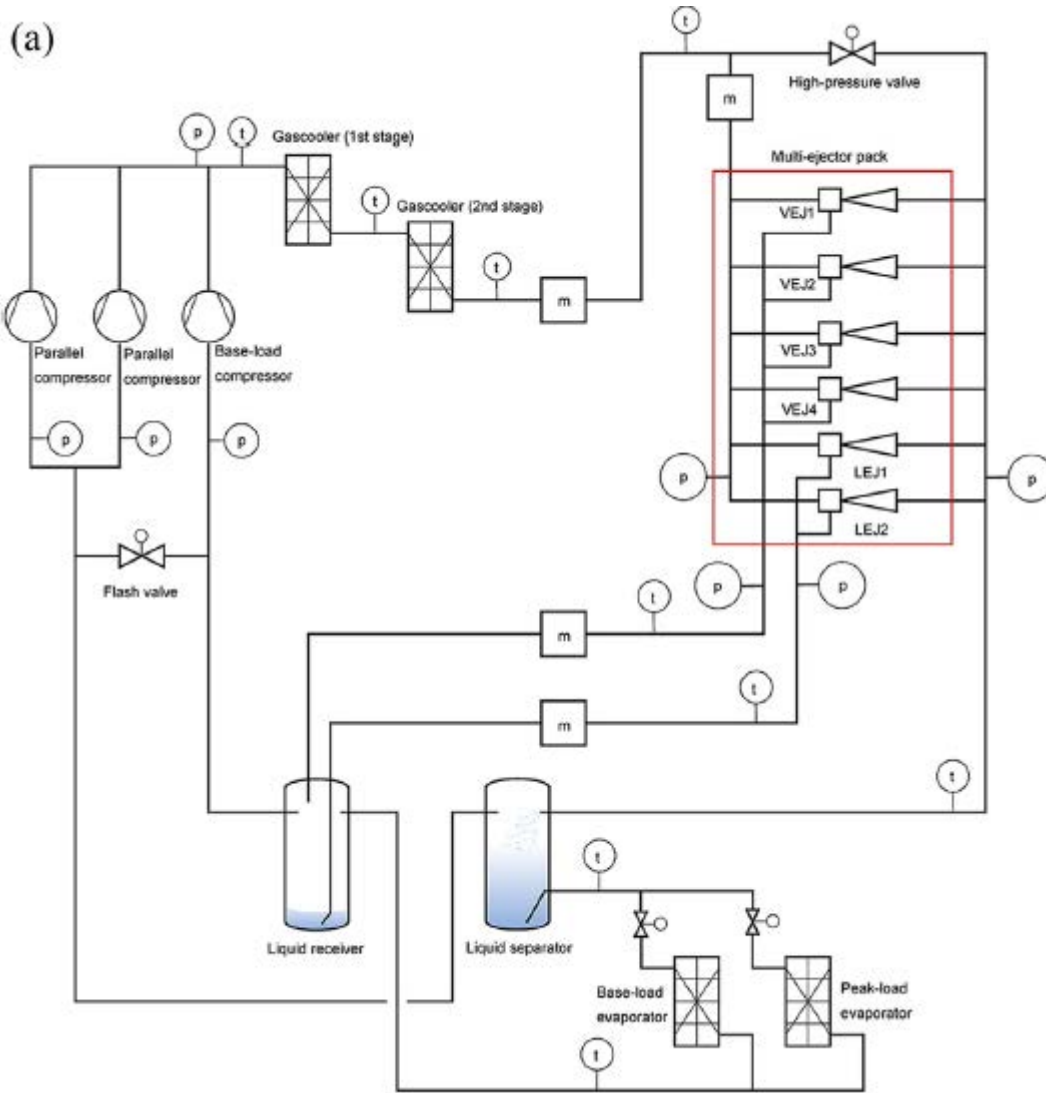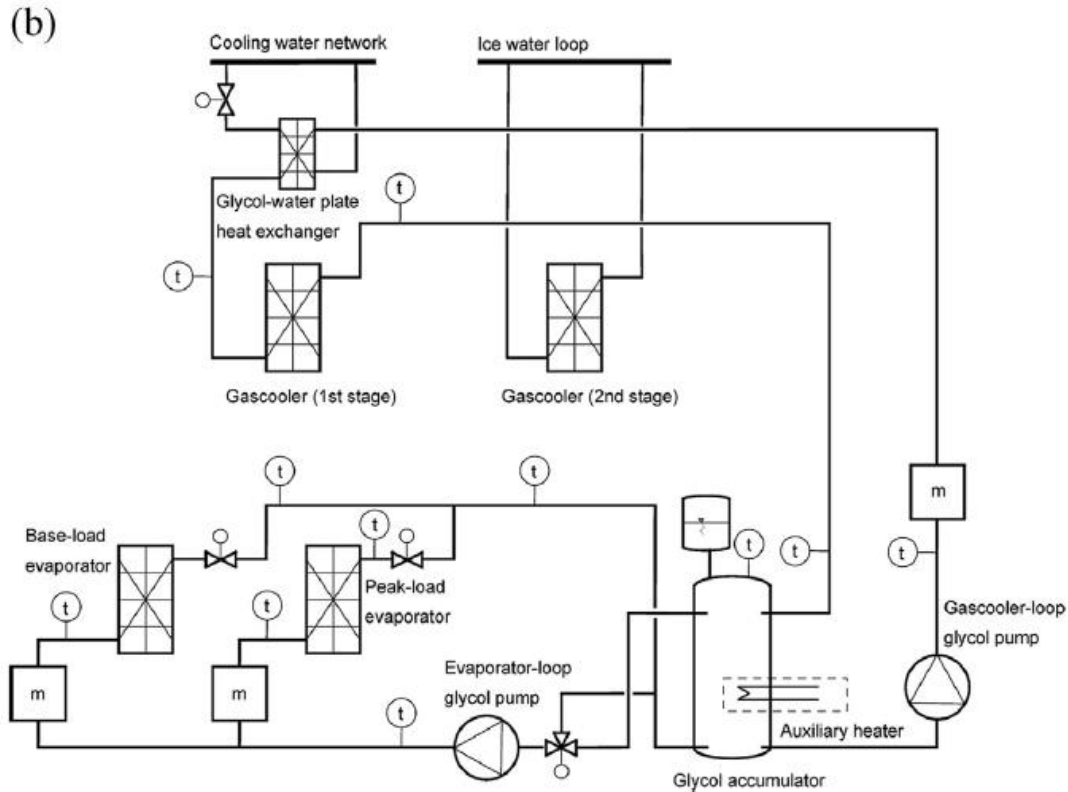
Fig. 11 Schematics of the multi-ejector test facility: (a) R744 circuit, (b) Glycol circuit. Instrumentation signatures: t-temperature sensor, p-absolute pressure sensor, m-mass flow rate meter[]

The ejector efficiency as defined by Elbel and Hrnjak[26] (2008) as a function of the motive nozzle inlet conditions and pressure ratios was mapped for vapor ejector 1. It indicated that to utilize a given ejector geometry in the optimum way, one should adjust the floating pressure ratio (or pressure lift) according to the heat sink conditions in the gas cooler. Besides, since each ejector cartridge may provide an individual performance map of unique features, by applying common boundary conditions to a series of parallel ejectors placed in operation, the overall system performance should be maximized because it is not possible to optimize individual ejector operations simultaneously.

System's response to a rapid change in load and ambient temperature for the HPV operation mode and HPV-assisted multi-ejector operation mode was presented. Profiles of the discharge pressure control error were also recorded for both alternative options. The results show that the overall system performance can be enhanced by the effects of the expansion work recovery. The percentage of the mass flow rate expanded through the multi-ejector block registered during these tests was high and varied between 84% and 96%.

Finally, the effects of parallel ejectors operation on the overall multi-ejector pack efficiency as well as expected improvement of the overall COP due to the use of expansion work recovery was examined and verified. The authors concluded that the

overall multi-ejector efficiency degraded gradually with the increasing mass flow rate expanded, implying intensified flow irreversibility in the pack. The registered values remained relatively high for almost the entire flow expanded in the pack. The system performance depended on a number of various parameters. Given the expansion work recovery invoked and consequent transfer of the load from the base-load compressors group to the parallel compressors group, it does not deteriorate the overall efficiency of the compressor pack. Correct usage of the multi-ejector block could maximize not only the effects of expansion work recovery but also the overall system performance shall take into account individual characteristics of the system components.

2.4 Conclusions

In this chapter, the background of reimplementation of CO_2 as an environmentally-friendly refrigerant is described. Several approaches applying CO_2 in supermarket refrigeration systems and compressor packs are presented in order to show the state-of-the art of this technology. A newest refrigeration system with multi-ejectors is introduced in detail. The compressor pack studied in this thesis is similar to the parallel compressor system with multi-ejector. Some of the results from this thesis should be applicable to the existing multi-ejector system to optimize its performance.

3 Numerical model description

3.1 Ejector supported R744 refrigeration system model (case study)

In order to set up a numerical model, a simple two stage compression cycle should be set up at the beginning. This system contains three sets of compressors, a set of ejectors, three heat exchangers, two throttling valves and two separators. A set of compressors are applied. The schematic diagram of the structure of this model is shown in figure 12.

The first loop is a typical gay cycle with two phase ejectors, an evaporator and a LT receiver. The LT stage (blue pipes) is connected to the MT separator to evaporate part of outlet liquid of ejector, while the MT stage compress the gas to the high side. Parallel compressors are used to suck the flash gas in the MT separator, and a bypass valve is used for keeping the pressure difference between LT reservoir and MT sepeator when the cooling load is 10% or less. The discharge of the LT compressors can be connected to either the MT separator or the LT receiver. If it is connected to the MT separator, the LT compressor outlet gas evaporates part of the liquid from the ejectors' outlet, while if connected to the LT receiver, it superheats the gas from the MT evaporator outlet. The state points are numbered in the following figure from 1 to 19, and represent the different thermodynamic states.
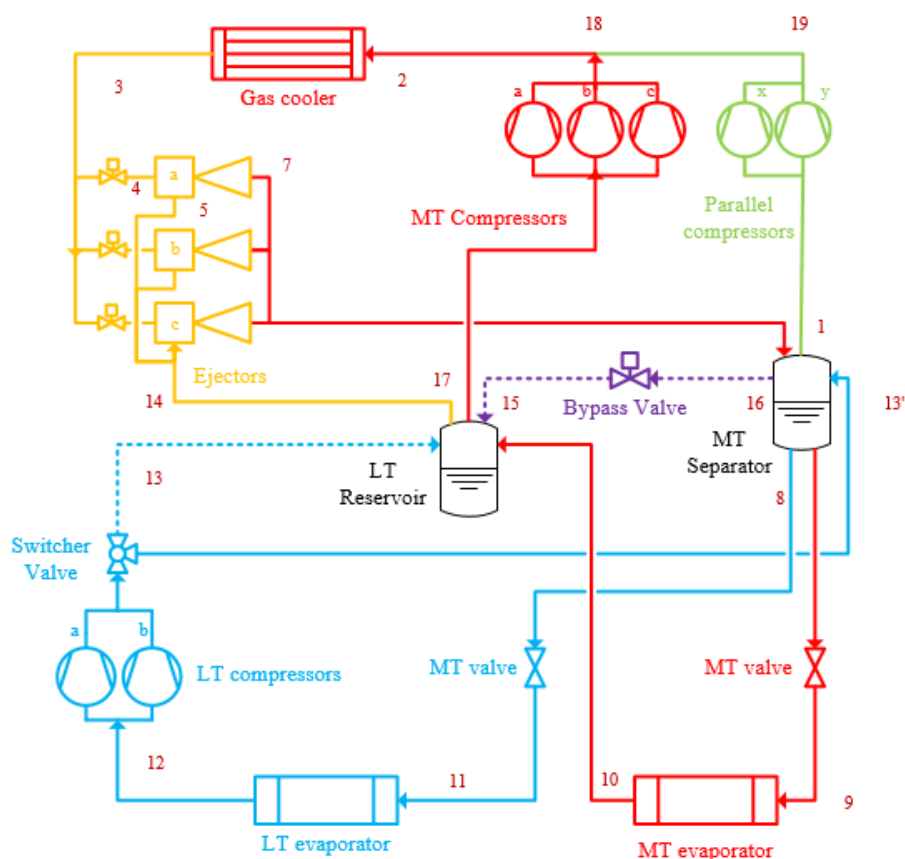
Fig. 12 A simple model of two-step compression R744 refrigeration cycle with ejectors

3.1.1 Parameters and equations in case study

To build up a numerical model, process equations and parameters during calculation are described in following equations. There are 4 pressure levels in the model, P_{high}, P_{medium}, $P_{intermediate}$ and P_{low}, which are high side pressure, medium pressure, intermediate pressure and low pressure level, respectively. Thus the pressure ratios of MT, AC (PA in the simple case) and LT sides are expressed in equation 3.1 to 3.3.

$$\pi_{MT} = \frac{P_{high}}{P_{medium}} \tag{3.1}$$

$$\pi_{AC} = \frac{P_{high}}{P_{intermediate}} \tag{3.2}$$

$$\pi_{LT} = \frac{P_{intermediate}}{P_{low}} \tag{3.3}$$

The compressor isentropic efficiencies are defined then in equation 3.4, where "i" represents MT, AC or LT, $h_{i,is,comp,out}$ and $h_{i,comp,out}$ stand for the isentropic outlet enthalpy of compressor and real outlet enthalpy of compressor, respectively. $h_{i,comp,in}$ stands for the inlet enthalpy of compressor.

$$\eta_{i,comp} = \frac{h_{i,is,comp,out} - h_{i,comp,in}}{h_{i,comp,out} - h_{i,comp,in}} \tag{3.4}$$

Formulas used for simulating the ejector are presented in equation 3.5, where $\dot{m}_{sn}$, $\dot{m}_{mn}$ are the mass flow rates in the ejector suction and motive nozzles, respectively. $h_{sn,out}$ and $h_{sn,in}$ stand for the enthalpies at the inlet and outlet of the suction nozzle, and $h_{mn,out}$, $h_{mn,in}$ for the enthalpies at the inlet and outlet(mixing chamber of ejector) of the motive nozzle.

$$\eta_{ejector} = \frac{\dot{m}_{sn}}{\dot{m}_{mn}} \cdot \frac{h_{sn,out} - h_{sn,in}}{h_{mn,out} - h_{mn,in}} \tag{3.5}$$

The cooling capacity of MT, LT and AC sides are shown in equation 3.6, where $\dot{m}_{i,evap}$ is the refrigerant mass flow rate of each evaporator, $h_{i,evap,out}$ and $h_{i,evap,in}$ are outlet and inlet refrigerant enthalpy of each evaporator.

$$\dot{Q}_{i,c} = \dot{m}_{i,evap} \left(h_{i,evap,out} - h_{i,evap,in} \right) \tag{3.6}$$

To simulate the operation point, two more sets of equations are defined as fundamentals. One is the equation group (3.7) of mass flow, the other is the equation group of energy balance (3.8). In these equations $\dot{m}_{ejector}$ and $\dot{m}_{i,comp}$ represent the total mass flow per ejector and mass flow per compressor, respectively, $h_{gc,out}$ stands for outlet refrigerant of gas cooler and $h_{ej,out}$ stands for the enthalpy at the outlet of the ejector.

$$
\begin{aligned}
\dot{m}_{ejector} &= \dot{m}_{mn} + \dot{m}_{sn} \\
\dot{m}_{sn} + \dot{m}_{MT,comp} &= \dot{m}_{MT,evap} \\
\dot{m}_{ejector} &= \dot{m}_{PA,comp} + \dot{m}_{MT,evap}
\end{aligned}
\tag{3.7}
$$

$$
\begin{aligned}
\dot{m}_{ejector} \cdot h_{ej,out} &= \dot{m}_{mn} \cdot h_{gc,out} + \dot{m}_{sn} \cdot h_{sn,in} \\
\dot{m}_{sn} \cdot h_{sn,in} + \dot{m}_{MT,comp} \cdot h_{MT,comp,in} &= \dot{m}_{MT,evap} \cdot h_{MT,evap,out} \\
\dot{m}_{ejector} \cdot h_{ej,out} + \dot{m}_{LT,evap} \cdot h_{LT,evap,out} &= \dot{m}_{LT,evap} \cdot h_{LT,evap,in} + \dot{m}_{PA,comp} \cdot h_{PA,comp,in} + \dot{m}_{MT,evap} \cdot h_{MT,evap,in}
\end{aligned}
\tag{3.8}
$$

Acquiring all the parameters above, the COP of each side is defined and obtained through equation 3.9 and 3.10. The total energy consumption can also be determined with equation 3.11, where (i=LT, MT and PA)

$$COP_{MT} = \frac{\dot{m}_{MT,evap} \cdot (h_{MT,evap,out} - h_{MT,evap,in})}{\dot{m}_{PA,comp} \cdot (h_{PA,comp,out} - h_{PA,comp,in}) + \dot{m}_{MT,comp} \cdot (h_{MT,comp,out} - h_{MT,comp,in})} \qquad (3.9)$$

$$COP_{LT} = \frac{\dot{m}_{LT,evap} \cdot (h_{LT,evap,out} - h_{LT,evap,in})}{\dot{m}_{LT,comp} \cdot (h_{LT,comp,out} - h_{LT,comp,in})} \qquad (3.10)$$

$$W_{total} = \sum_{i=1}^{n} \dot{m}_{i,comp} \cdot (h_{i,comp,out} - h_{i,comp,in}) \qquad (3.11)$$

3.1.2 Setting up the library of compressors

Firstly, a library of compressors should be established. The compressors for the MT loop and LT loop were chosen separately. The initial parameters are listed in table 1.

Table 1 Initial Parameters for Compressors

Initial Conditions	
MT evaporation temperature	-2 ℃
LT evaporation temperature	-30 ℃
MT cooling capacity	60 kW
LT cooling capacity	10 kW
Gas cooler outlet temperature	35 ℃

According to the initial input parameters, each compressor type and its power input were specified. The input and output parameters, which were used to calculate efficiencies, were also integrated. The parameters of the correlations to calculate this efficiencies, together with compressor, are listed in table 2, where π (or PI) stands for pressure ratio.

Table 2 Compressor efficiency information

Type	Isentropic efficiency a1+a2*PI+a3*PI^2+a4*PI^3+a5*PI^4				
	a1	a2	a3	a4	a5
CD1400H	0.5258	0.1065	-0.0175	7.00E-19	-3.89E-20
CD1000H	0.5225	0.1044	-0.0171	-2.80E-18	1.74E-19
CD380H	0.388	0.2091	-0.0591	0.0043	-2.45E-20

For the MT, Parallel and LT compressor sets, three types of compressors were chosen separately, namely "CD1400H", "CD1000H" and "CD380H". All of them are semi-hermetic reciprocating compressors. Their efficiency data, both isentropic efficiency and volumetric efficiency can be obtained from Pack calculation software, designed by Denmark Technical University.

The efficiencies of each compressors are calculated and illustrated in the form of fitted curves, and then the linear compressor efficiency equation was incorporated into the system equations to meet the variable boundary conditions. Figure 13 shows the fitted isentropic efficiency curves of the three compressor types. The highest efficiencies occur with pressure ratios between 2 to 3.5.
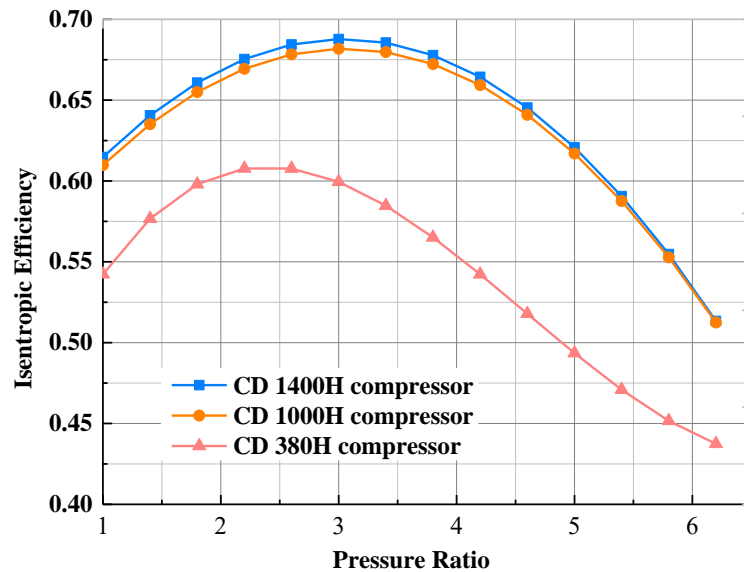
Fig. 13 Isentropic efficiency curves of chosen compressors

3.2 Numerical model modification for a comprehensive case

Based on the case study in the last section, a more comprehensive model, with parallel compressors applicable for both AC and MT side, is made to show the performance and energy consumption in a real case. An AC evaporator is added to make PA compressors used for air conditioning.

It is a possibility of cooling load distribution in a small centralized supermarket that 60 kW is consumed by MT cooling cabinets, less than 50kW for air conditioning and about 10 kW for LT freezer. To cover the cooling load with steps such as from 5%-30%, a more specific compressor library was set up. The compressors were chosen from Dorin CO_2 compressor series. As mentioned in table 1, the assumed MT cooling capacity is 60 kW, thus the required minimum cooling load is subsequently 3 kW-18 kW. Therefore, the minimum MT cooling load should at least be covered by the minimum-sized single compressor, and the maximum cooling load should be covered when all of the compressors work at their rated rpm.

The total number of compressors that can be implemented on the compressor rack should be as low as possible. The desirable number of first try is to use 4 compressors with only 2 converters according to current lab condition, which allows the compressors to operate between the minimum frequency 30 Hz and the maximum frequency 65 Hz.

Thus the previous system diagram should be modified, including the arrangement of compressors and AC system. The modified system diagram is shown in figure 14.
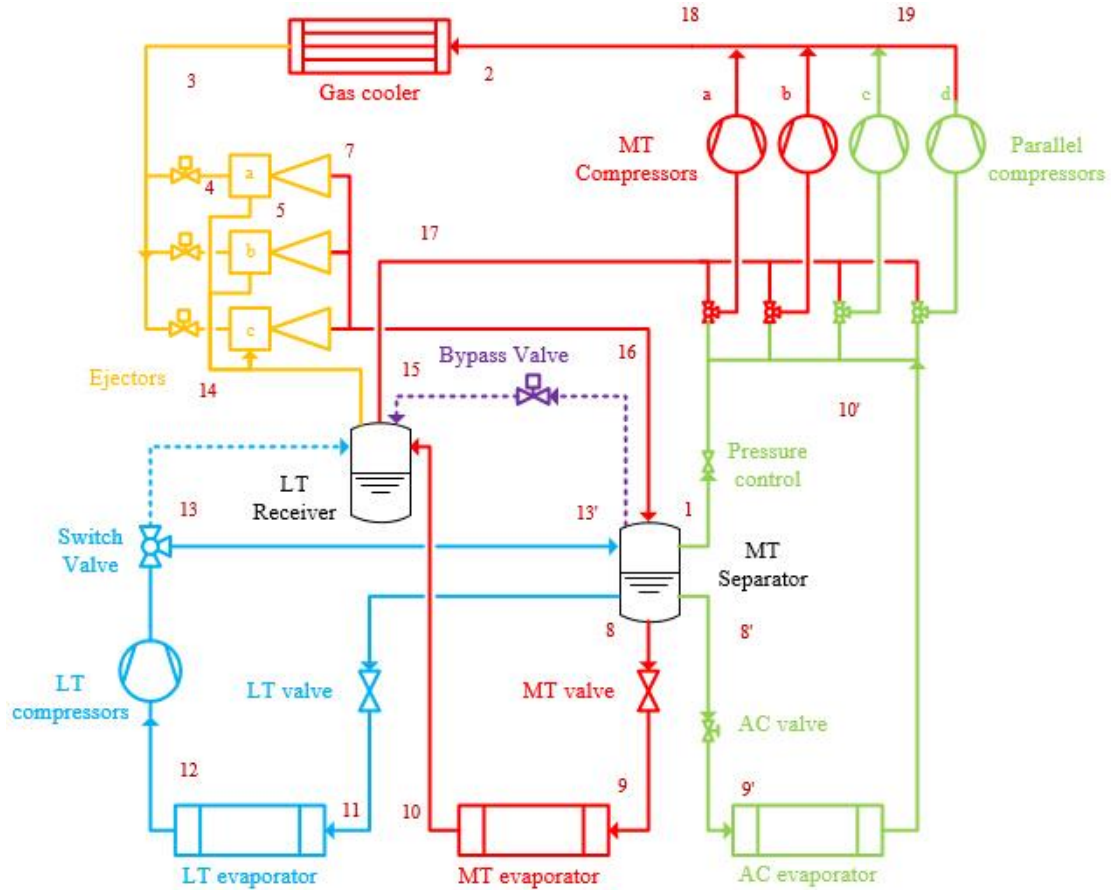
Fig. 14 Modified R744 compressor pack with multi-ejectors and AC evaporator

There are 2 suction lines in the system, which allows the compressors to be allocated independently for MT and AC side. Besides, in order to make the AC loop work without pump, 2 valves with a pressure drop of 0.5 bar were implemented between AC evaporator and MT separator and between the AC suction line and MT separator.

3.2.1 Parameters and equations for the modified model

For the modified model, the expression equations of COP of each side is different from the simple case for the reason that the MT and PA compressors are now allowed to switch to the other suction and the energy consumption of each side is also different due to the load taken by the different compressors and ejector. The COPs are shown in equations 3.12-3.14.

$$COP_{MT,revised} = \frac{\dot{m}_{MT,evap} \cdot (h_{MT,evap,out} - h_{MT,evap,in})}{\dot{m}_{MT,comp} \cdot (h_{MT,comp,out} - h_{MT,comp,in}) + \dot{m}_{SN} \left[(h_{SN,out} - h_{SN,in}) + (h_{AC,comp,out} - h_{AC,comp,in}) \right]} \quad (3.12)$$

COP of AC is simply expressed as AC evaporator cooling capacity over AC compressor power consumption.

$$COP_{AC} = \frac{\dot{m}_{AC,evap} \cdot (h_{AC,evap,out} - h_{AC,evap,in})}{\dot{m}_{AC,comp} \cdot (h_{AC,comp,out} - h_{AC,comp,in})} \quad (3.13)$$

COP of LT is expressed as AC evaporator cooling capacity over the power consumption of LT and AC compressor caused by refrigerant in LT loop.

$$COP_{\text{LT,revised}} = \frac{\dot{m}_{\text{LT,evap}} \cdot (h_{\text{LT,evap,out}} - h_{\text{LT,evap,in}})}{\dot{m}_{\text{LT,evap}} \cdot \left[(h_{\text{LT,comp,out}} - h_{\text{LT,comp,in}}) + (h_{\text{AC,comp,out}} - h_{\text{AC,comp,in}}) \right]} \tag{3.14}$$

In equations 3.12-3.14, $\dot{m}_{\text{MT,evap}}$, $\dot{m}_{\text{AC,evap}}$, $\dot{m}_{\text{LT,evap}}$ stand for the mass flow rates of refrigerant in each evaporator (MT, AC, and LT); $\dot{m}_{\text{AC,comp}}$, $\dot{m}_{\text{MT,comp}}$, $\dot{m}_{\text{SN}}$ are the mass flow rates of refrigerant at AC and MT compressors, as well as suction nozzle; $h_{\text{MT,comp,out}}$, $h_{\text{MT,comp,in}}$, $h_{\text{AC,comp,out}}$, $h_{\text{AC,comp,in}}$, $h_{\text{LT,comp,out}}$, $h_{\text{LT,comp,in}}$ are inlet and outlet enthalpy of each compressor; $h_{\text{MT,evap,out}}$, $h_{\text{MT,evap,in}}$, $h_{\text{AC,evap,out}}$, $h_{\text{AC,evap,in}}$, $h_{\text{LT,evap,out}}$, $h_{\text{LT,evap,in}}$ the enthalpies at the inlet and outlet of each evaporator; $h_{\text{SN,out}}$ and $h_{\text{SN,in}}$ are the enthalpies at the inlet and outlet area (mixing chamber of the ejector) of suction nozzle.

3.2.2 Compressor Library and Input Matrix

To select the compressors that fit the limit of the number of compressors, one operation condition is preset: MT evaporation temperature -2 °C and gas cooler outlet temperature 35 °C. An input matrix consists of a series of compressors with the data of the cooling capacities. The specific cooling capacity, displacement and rpm rate of the compressors are listed in table 3, which offered a reference for investigating the possible compressor combination arrangements.

Table 3 Input Matrix for -2 [C], 35 [C]

Size	MIN Capacity [kW]	MAX Capacity [kW]	Capacity @50Hz [kW]	Varified range [kW]	MIN Displacement [m^3/h]	MAX Displacement [m^3/h]	Displacement @50Hz [m^3/h]
CD180H	1.67	3.32	2.62	1.65	0.67	1.46	1.12
CD300H	2.27	4.51	3.55	2.24	0.88	1.90	1.46
CD350H	3.02	5.99	4.72	2.97	1.13	2.44	1.88
CD360H	3.90	7.73	6.09	3.84	1.43	3.11	2.39
CD380H	4.85	9.63	7.58	4.78	1.80	3.90	3.00
CD700H	7.14	14.16	11.15	7.02	2.60	5.64	4.34
CD750H	7.74	15.37	12.10	7.62	2.84	6.16	4.74
CD1000H	9.36	18.58	14.63	9.21	3.37	7.29	5.61
CD1200H	11.62	23.05	18.15	11.44	4.15	9.00	6.92
CD1300H	15.01	29.79	23.46	14.78	5.35	11.60	8.92
CD1400H	15.48	30.72	24.19	15.24	5.69	12.32	9.48
CD1500H	17.26	34.25	26.97	16.99	6.07	13.16	10.12
CD1900H	19.74	39.17	30.84	19.43	6.97	15.11	11.62
CD2000H	19.37	38.44	30.26	19.07	7.01	15.20	11.69
CD2400H	23.13	45.90	36.14	22.77	8.30	17.99	13.84
CD2500H	26.03	51.65	40.67	25.62	9.43	20.44	15.72
CD3000H	30.01	59.54	46.88	29.54	10.70	23.19	17.84
CD3400H	34.31	68.09	53.61	33.78	12.15	26.33	20.25
CD3500H	38.66	76.71	60.40	38.05	13.95	30.23	23.25

Several logic lines should be taken into consideration:

1) The minimum size compressor (compressor 1) should be connected to a converter to operate and cover the minimum cooling load continuously;

2) The maximum capacity of the second smallest compressor (compressor 2) should be a bit less than the smallest one in order to overlap a part of the load in case that compressors are turning on and off frequently. It is supposed to get the other converter.

3) The second largest (compressor 3) and the largest compressor (compressor 4) are going to be operated at 50 Hz, thus the rate capacity of compressor 3 should be a bit less than the overall capacity of compressor 1 and 2. Compressor 4 should at least have a capacity at least large enough to reach the overall capacity 100 kW.

3.3 Conclusions

In this chapter, a numerical model for simple case study and a modified model for comprehensive simulation are build up respectively. The system structures are illustrated first. The equations and corresponding parameters utilized in these equations, as well as compressor library are set up for the simple case. The compressor library of the modified model, several assumptions that specify the limitations of calculation, and calculation procedure including logic design and revised COP expressions are presented subsequently.

The system description and equation explanations are presented as how the calculation is conducted and why is the calculation implemented in this way. The calculation result and relevant analysis is shown in chapter 4.

4 Simulation results and analysis

4.1 Case study
4.1.1 Calculation result and analysis
For a specific scenario, several input parameters including LT cooling capacity and MT cooling capacity were chosen according to a test case similar to those in the line of research of Professor Hafner. Additionally, the ejector efficiency and compressor efficiency curves are also incorporated in the numerical model.

The calculation process was conducted through EES. The steady-state ejector calculations were based on the basic ejector principle of Elbel (2007). The recovered energy from the motive flow pumps the suction gas to the diffuser pressure. The mixed fluid is two-phase flow. The ejector efficiency is fixed at 0.3 and the pressure lift is defined as 9 bar.

Once incorporated all the efficiency polynomials into the ESS code, we can get the system logp-h diagram, a set of results showing the mass flow changing with different pressure ratio level, as well as the optimized COP variation with different high side pressure and cooling capacity. The system logp-h diagram was made with the results obtained from equations and is shown as figure 15.
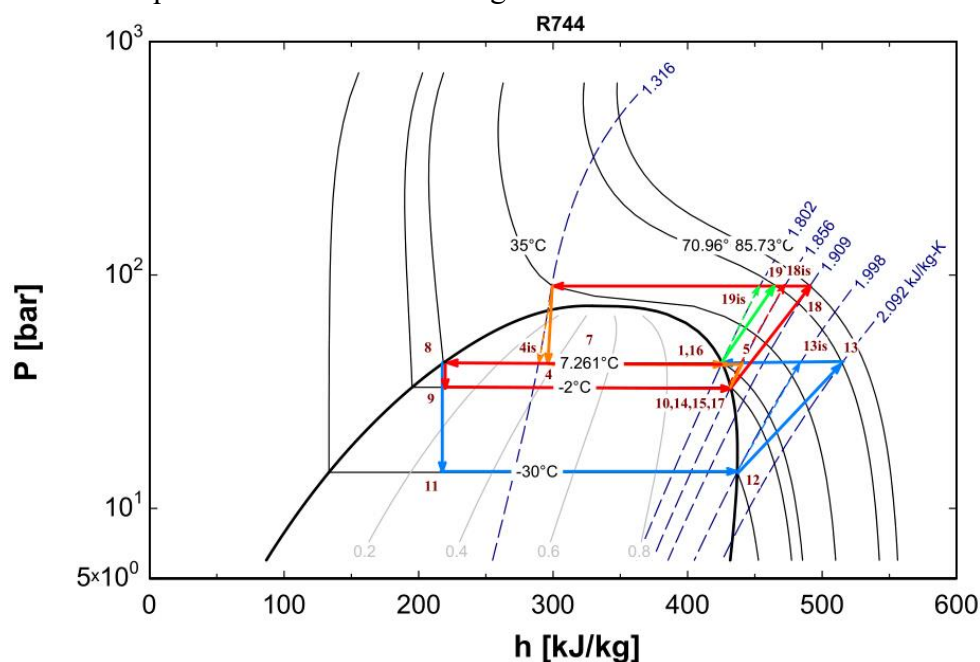
Fig. 15 Log p-h diagram of the two-step refrigeration system with ejector

Figure 16 illustrates the mass flow rates through the most important components as a function of the ejector pressure lift. It can be seen that the mass flow rates change towards different direction. The red line in the graph shows indicates the 0 mass flow rate level (regard the direction same as system arrangement as positive). It is clear that when the pressure lift is less than 8 bar, the mass flow rate of MT compressor is negative. Because the sum of mass flow rate of MT compressor and the mass flow rate of ejector

suction nozzle is constant as equal to the mass flow in MT evaporator. Thus this mass flow rate can be maintained to a positive value only by reducing the inlet mass flow of suction nozzle. Better ejector pressure lift is required in this case for adjustment. This arrangement transfer part of load from MT compressors and to Parallel compressors. The influence of pressure lift on mass flow rates is significant because it has further effects on system COP.
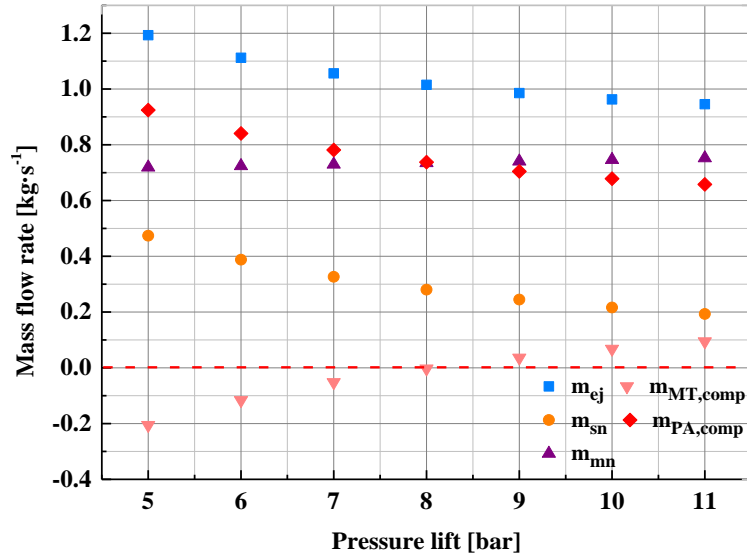
Fig. 16 Mass flow rates through the most important components with pressure lift

Under the constant preset gas cooler outlet temperature, the COP of the MT part has a maximum value when the high side pressure ranges from 80 bar to 92 bar, as is seen in figure 17. With the ambient temperature of 35 °C, the maximum MT COP is around 1.9. At the same time, this diagram shows that when the ambient temperature is fixed, the COP_{MT} is not strongly influenced by the high side pressure (the COP changes during the pressure range less than 0.1).
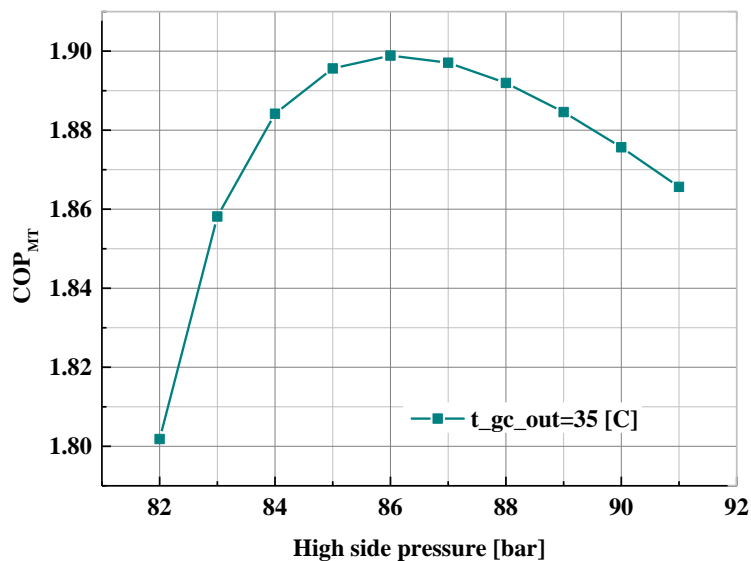
Fig. 17 COP_{MT} variation with high side pressure at constant ambient temperature

Figures18 and 19 show the COP variation with high side pressure at different ambient temperatures (gas cooler outlet temperatures), and with gas cooler outlet temperature at different high side pressure. From figure 18, we can see that COP rises as the temperature gets higher, reaches a maximum and then falls down gradually. Thus, under the assumptions of such system, each ambient temperature has a corresponding optimal high side pressure. The trend of maximum COPs is marked with a red dashed-line for further calculation and verification. Besides, the COP changing range reflects that ambient temperature has a great influence on it. This statement can be clearly seen in figure 19. Additionally, it illustrates another point that the COP varies more dramatic when high side pressure is lower and for each ambient temperature, the optimized high side pressure can be clearly seen.
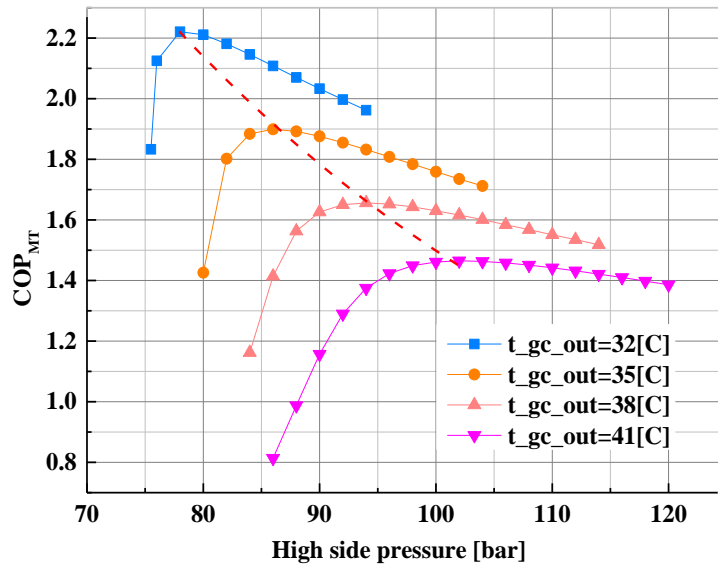
Fig. 18 COP$_{MT}$ variation with high side pressure at different gas cooler outlet temperatures
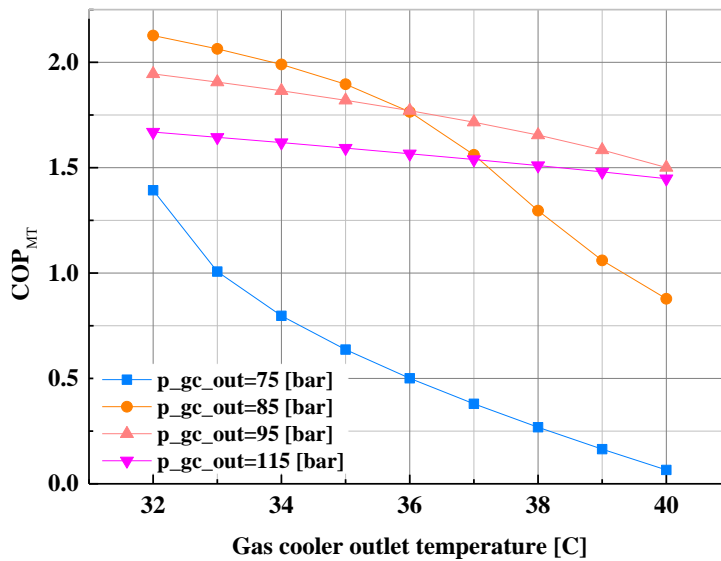
Fig. 19 COP$_{MT}$ variation with gas cooler outlet temperature at different high side pressures

Except for gas cooler outlet temperature and pressure, the cooling capacity of LT evaporator and MT evaporator also affect MT COP. Isometric COP diagram figure 20 shows the mapping of COP changing with different LT and MT cooling capacity with optimized gas cooler outlet temperature 35 °C and pressure 86 bar. It's obvious that MT COP is very sensitive to MT cooling capacity, it is also apparently affected by LT capacity.
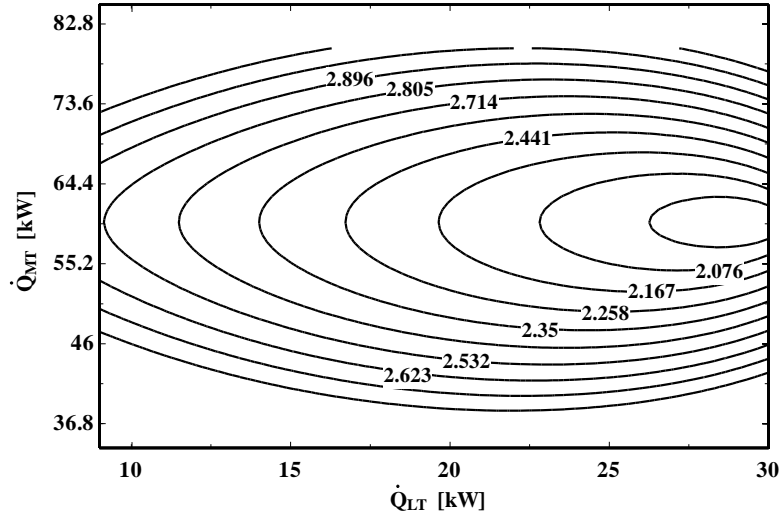
Fig. 20 MT COP variation with MT & LT cooling capacity

In addition to MT COP, the energy consumption is also a frequently discussed parameter. Figure 21 is a color band diagram showing the energy consumption distribution according to the high side pressure and gas cooler outlet temperature of the system. The black arrows represent the gradient of consumption. It is obvious that the energy consumption increases drastically when gas cooler outlet temperature and pressure are both at high level.
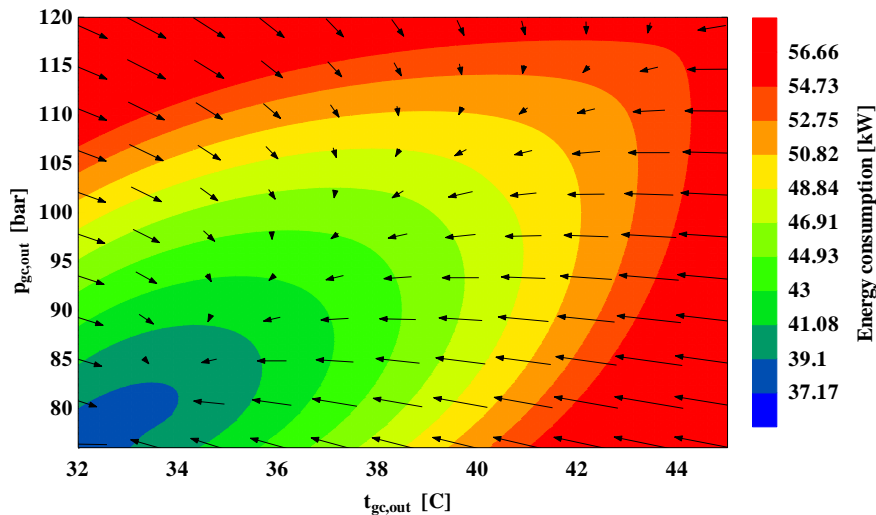
Fig. 21 Energy consumption variation with ambient temperature and high side pressure

4.1.2 Conclusion and prospect

According to the analysis above, the following conclusions can be made, for this two stage compression refrigeration system with ejectors:

1. Each operation condition has a corresponding balance point. For fixed MT cooling capacity the MT evaporator outlet pressure and temperature are fixed (assume no superheat), which means that if the ejector is able to transfer more vapor from the LT accumulator side towards the pressure level of the MT separator, the pressure set point of the PA compressor should be changed (increased). Otherwise, the ejector removes more vapor from the LT accumulator which results in lower evaporation temperatures, even without the MT compressors in operation.

Therefore, at the assumed cooling capacity, ambient condition and evaporator temperatures, the MT side can work properly either when using ejectors with lower efficiency or if the pressure lift is adjusted in case of 100% ejector vapor suction from the MT side.

2. Each ambient temperature has a corresponding optimized operation high side pressure.

The COP of the MT circuit reaches an optimum and then falls down gradually at a fixed high side pressure as ambient temperatures are increasing. This means the refrigeration system has an optimum high side pressure for each ambient temperature (gas cooler outlet temperature). The trend of optimum pairs of conditions can be marked with a line to show the system COP with certain ambient temperature and its optimum high side pressure. The COP changing range reflects that ambient temperature has great influence on it. This means when the high side pressure is relatively low, the COP of the MT loop is more sensitive to the temperature change.

3. The energy consumption at certain ambient temperature and high side pressure can be integrated in a band diagram, from which we can see the minimum energy consumption at each high side pressure by color and the corresponding ambient temperature range (band width). Thus the minimum energy consumption at certain ambient temperature and its optimum high side pressure can be estimated.

However, a more specific compressor library should be set up, including information of compressor size, rpm, real frequency efficiency as well as different combination of compressors with varied capacity, to cover the cooling load with steps such as from 5%-30%. An input matrix including cooling capacities, ambient and evaporator temperature should be set up additionally. The compressor rpm efficiency data should also be defined and incorporated into the code to conduct semi dynamic calculation. More arrangements should be discussed to find which combinations (combined compressor sizes) are best for minimizing energy consumption (taking into account compressor part load efficiency) and maximizing COP. Besides energy consumption

and COP variation with changing cooling capacity and compressor rpm, part load efficiencies should be considered.

Hence, the subsequent work is a logic strategy to operate compressor racks according to different cooling loads, in order to minimize energy consumption and optimize system COP, as well as covering the cooling load curve as smoothly (each % load from 5-100% cooling load) as possible. Additionally, the compressor efficiency experiments should be conducted to find the possibility to substitute one or two of the compressors applied in the simulation work. The model with the tested compressor serves as a reference system and it will be compared with the previous system. The COP and Energy consumption will be specified according to the two system with same ambient and load conditions.

4.2 Comprehensive simulation
4.2.1 Case study for compressor capacity calculation based on MT load
To investigate how should the selected compressors be arranged, either to MT or to AC, with converter or not, an example was studied. This example only allows the compressors to be operated in MT side. -2 °C was assumed as evaporator temperature, and 35 °C for gas cooler outlet temperature. Based on the logic lines explained in section 3.2.2, four compressors were chosen, and listed in table 4.

Table 4 Selected compressors

Compressor naming	
Compressor 1	CD750H
Compressor 2	CD1300H
Compressor 3	CD2400H
Compressor 4	CD1900H

According to the logic line above, the strategy including the compressors in operation with their capacity combination is illustrated in figure 22. It shows how this strategy covers the cooling load from around 8% to 100% capacity. The hollow bars represent the changeable capacities, while the solid bars mean the rate capacities. The compressor displacements are also listed for the corresponding compressors. The displacement data is applicable in the numerical model for mass flow calculation and compressor efficiency. In this case, it is clear that if 2 converters are arranged in either MT side or AC side, the cooling load can be easily covered by 4 compressors with 2 converter. In other words, the maximum capacity of the smallest compressor is always larger than the minimum capacity of the largest compressor, or compressor combination.
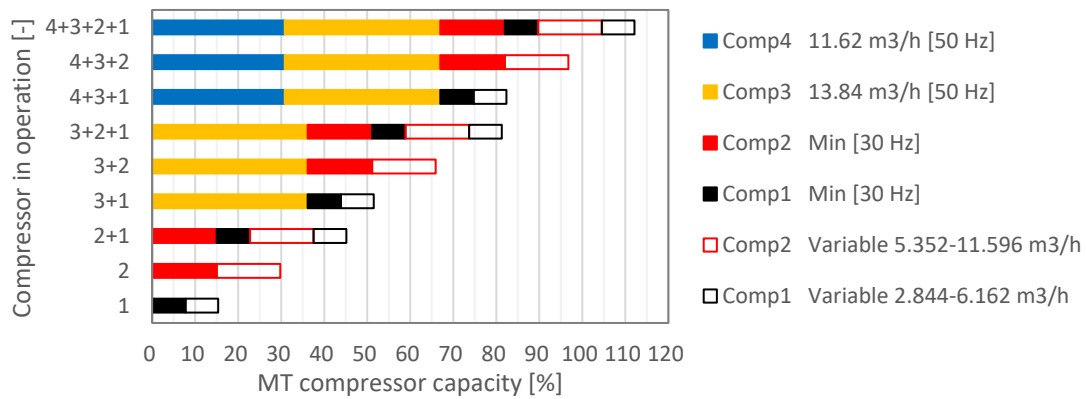
Fig. 22 Compressor arrangement strategy for the case that only has MT system in operation

4.2.2 Case study for compressor capacity calculation based on both MT and AC loads

In real cases, the compressors are only allowed to operate at frequencies among 30 Hz-65 Hz, and except for refrigeration, part of the load comes from air conditioning. Taking into account an AC load around 40 kW, the load range should be widened to 8%-100% (total load around 100 kW). According to the example above, the load is supposed to be covered in a way that uses 4 compressors and 2 converters for frequency adjusting, the load range should also be covered as smoothly as possible.

To achieve this goal, new logic lines should be recognized and specified first.
1) A new set of compressors should be selected in the new case. The two converters are also supposed to be installed on different compressors.
2) Evaporator temperature -2 ℃ and ambient temperature 35 ℃ are set as design point. The capacity range of selected compressors should be specified.
3) The two compressors with converters should be arranged separately on MT side and AC side, otherwise the capacity of either of the 2 sides cannot be adjusted in real cases.
4) It is impossible to cover the AC and MT load smoothly at the same time, which means either or both of them have gaps in operation. These gaps were identified during the identification of the best solution.

The compressor capacity data for the selected compressors were obtained from the product documents, as well as the correlation between capacity and frequency, which is linear between 30 Hz-65 Hz. Noticing that it is impossible to meet the cooling load of both sides at the same time, it is better to make one side fit the desirable conditions. In this case, AC load is covered smoothly. Given that the AC system is in operation, the pressure lift of the ejector cannot be too large to prevent that there is no refrigeration on AC side. Thus the diffuser pressure is assumed 40.04 bar according to previous calculation. According to the previous system introduction, the evaporating pressure and temperature for AC side are 39.54 bar and 4.9 ℃. The new compressors are chosen to approach this goal and their capacity data were listed in table 5.

Table 5 Input Matrix for AC and MT compressors

	AC 4.849[C], 35[C]							
Size	MIN Capacity [kW]	MAX Capacity [kW]	Capacity @50Hz [kW]	Varified range [kW]	MIN Displacement [m^3/h]	MAX Displacement [m^3/h]	Displacement @50Hz [m^3/h]	Indication
CD750H	9.547	18.945	14.917	9.398	2.84	6.16	4.74	Compressor 1
CD1200H	14.330	28.435	22.39	14.106	4.15	9.00	6.92	Compressor 3
CD1300H	18.530	36.770	28.953	18.240	5.35	11.60	8.92	Compressor 2
CD1400H	19.055	37.812	29.773	18.757	5.69	12.32	9.48	Compressor 4
	MT -2[C], 35[C]							
Size	MIN Capacity [kW]	MAX Capacity [kW]	Capacity @50Hz [kW]	Varified range [kW]	MIN Displacement [m^3/h]	MAX Displacement [m^3/h]	Displacement @50Hz [m^3/h]	Indication
CD750H	7.74	15.37	12.10	7.62	2.84	6.16	4.74	Compressor 1
CD1200H	11.62	23.05	18.15	11.44	4.15	9.00	6.92	Compressor 3
CD1300H	15.01	29.79	23.46	14.78	5.35	11.60	8.92	Compressor 2
CD1400H	15.48	30.72	24.19	15.24	5.69	12.32	9.48	Compressor 4

According to all the information collected and the calculations conducted, the real results including load gaps that cannot be covered completely and the minimum cooling load reachable with certain numbers of compressors and converters are specified in figure 23. This figure depicts the load that is able to be covered by AC and MT side, as well as the gaps in MT side. The hollow bars represent the adjustable capacity range. When more or larger compressors are allocated to AC side, then the adjustable range for MT would get less. The gaps that cannot be covered and the exact range were also listed in table 6. Additionally, the operation frequency and the corresponding displacement are listed in the legend, same as that in the case for only MT load.
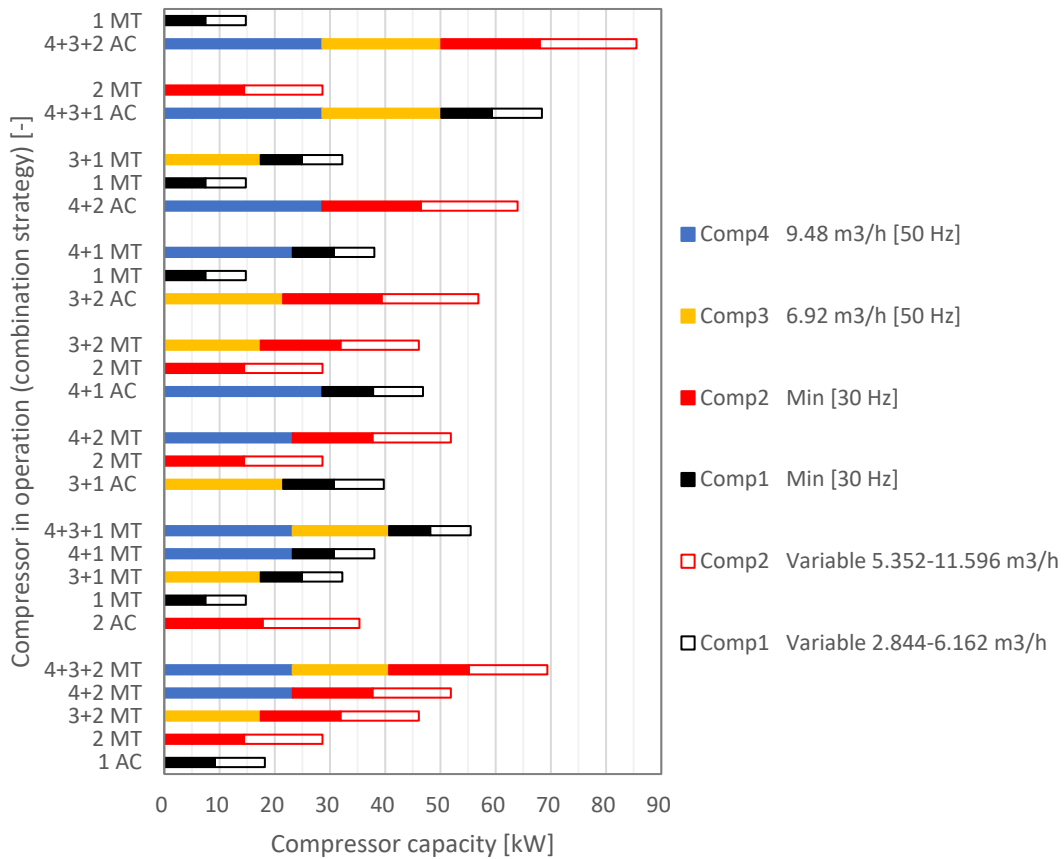
Fig. 23 Load covering strategy with 4 compressors and 2 converters for MT & AC

Table 6 MT gaps in different cases [kW]

MT Gaps	1 for AC	1 for AC	1 for AC	2 for AC	2 for AC
Where	2 to 3+2	3+2 to 4+2	4+2 to 4+3+2	1 to 3+1	3+1 to 4+1
Amount	3.24	-8.41	3.24	10.12	-1.53
Gap or not	YES	NO	YES	YES	NO
MT Gaps	2 for AC	3+1 for AC	4+1 for AC	3+2 for AC	4+2 for AC
Where	4+1 to 4+3+1	2 to 4+2	2 to 3+2	1 to 4+1	1 to 3+1
Amount	10.12	9.05	3.24	15.93	10.12
Gap or not	YES	YES	YES	YES	YES

Table 6 shows the gaps occurred in operation with the assumed conditions. From this table, it can be seen that the gaps are not very large, mostly less than 10 kW when less compressors are arranged to AC side. If larger compressors are allocated to AC, then the operation gaps for MT side would get larger (around 10 kW or more). Specifically, if compressor 1 is allocated to AC side, then there are 2 gaps on MT side. When compressor 3 is added to run parallel with compressor 2, 3.24 kW of cooling load cannot be covered. The same amount of 3.24 kW cooling gap occurs when compressor 3 is added for parallel operation with compressor 2 and 4.

When compressor 2 is used for AC side (higher load for AC side), the MT load gaps that cannot be covered occur in the same way as the case when only compressor 1 is used for AC side. The gaps exist when compressor 3 is added on compressor1, or on compressor 4 and 1. Both gaps are 10.12 kW.

As more compressor are allocated to AC side, the gap gets larger. The largest gap exists when compressor 2 and 3 are allocated for AC, and compressor 4 is added to operate with compressor 1. Due to the large capacity difference between the smallest and largest compressor, this gap is inevitable. Nevertheless, compared to the load which has already been covered, these load gaps can be considered acceptable. Besides, in the latter situation when ejector is applied, it takes some load from MT side, which means some of these gaps can be covered by ejector.

4.2.3 Assumptions and calculation preparation
Applying the load condition above, it is necessary to take 20 to 30 cases to identify how this compressor operation strategy improves the system performance.

To achieve this target, several assumptions were made:
1) The AC cooling load has a linear relation to the ambient temperature. It starts to appear at around 25 °C and reaches a maximum of 40 kW.
2) According to the previous system calculation, each gas cooler outlet temperature has a corresponding optimum high side pressure. It can be taken as a function, which is available by fitting the optimum points of the system. Note that there is a practical limitation of maximum pressure of 120 bar.
3) Considering the real performance of heat exchangers, the temperature difference between gas cooler outlet temperature and ambient temperature should have a linear correlation with the gas cooler load percentage.

According to assumption 1 and 2, it is much clear to show the correlation for ambient temperature with optimum high side pressure and AC cooling load. It is shown in figure 24. The fitted function is shown in formula (4.1) where $P_{gc, out}$ is outlet pressure of the gas cooler, t_{amb} is ambient temperature.

$$P_{gc, out}=a+b*t_{amb}+c*t_{amb}^2 \qquad (4.1)$$

In which,
a=33.5158 [bar];
b=0.7733 [bar/C];
c=0.0338 [bar/C^2].
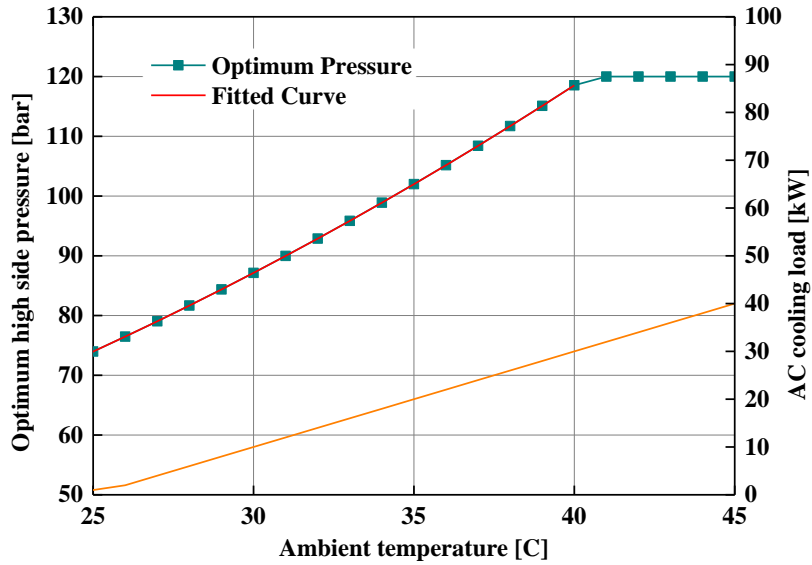
Fig. 24 Optimum high side pressure and AC cooling load as a function of ambient temperature

In the meantime, it is also critical to define the temperature difference between the ambient temperature and gas cooler outlet temperature, which is an important reference to define the gas cooler size. The correlation is assumed according to experience value of several supermarket as seen in equation 4.2, where Q represents for gas cooler load percentage and $t_{gc, out}$ represents for outlet temperature of the gas cooler. The initial value of Q is set to 1, shown in figure 25.

$$t_{gc, out}=t_{amb}+10*Q \tag{4.2}$$
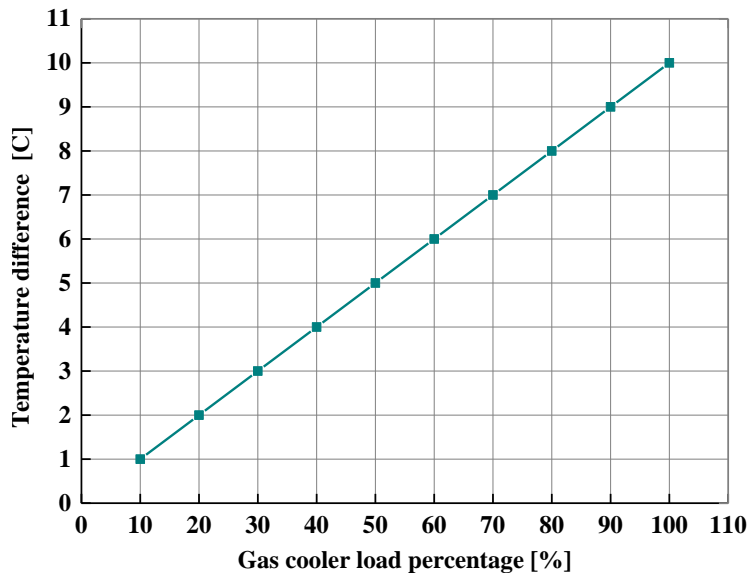
Fig. 25 Assumed temperature difference of gas cooler outlet temperature and ambient temperature according to gas cooler load percentage.

However, it is not feasible to apply this relation into calculation, for that the accurate load percentage needs to be confirmed through calculation with given gas cooler

temperature. Thus, it is necessary to use a logic loop to find the right value of gas cooler load percentage at first. The accuracy was set to 0.01 to ensure that the error of gas cooler load percentage would be as most 1%. With the proper high side pressure and exact gas cooler load, the outcomes such as COP for each side can be obtained more close to the real situation.

Besides, the MT evaporator temperature should also be adjusted. First, the ejector should not take too much load from MT side in case the mass flow rate of MT compressor becomes negative. Second, when the mass flow rates of MT compressors are too low to reach the minimum capacity of the smallest compressor implemented on MT side, then the MT compressor is supposed to be shut down by slightly increasing the MT evaporator temperature. This temperature should be set as the proper MT evaporator temperature in this situation. When MT load increases and reaches the minimum capacity, then MT compressor should be implemented back, then the temperature should turn back to initial value.

In the meantime, the Gas cooler loop and the temperature adjusting loop should be indicated, which means the two values should be obtained at the same time after the whole loop is called. The logic diagram is shown in figure 26, and it contains every step including the decision procedure, inputs and outputs. t_amb is ambient temperature; Q_dot_MT, Q_dot_LT, Q_dot_AC are MT, LT and AC cooling load; QL_MT is the left MT cooling load without the part taken by ejector; t_MT_evap is MT evaporator temperature.
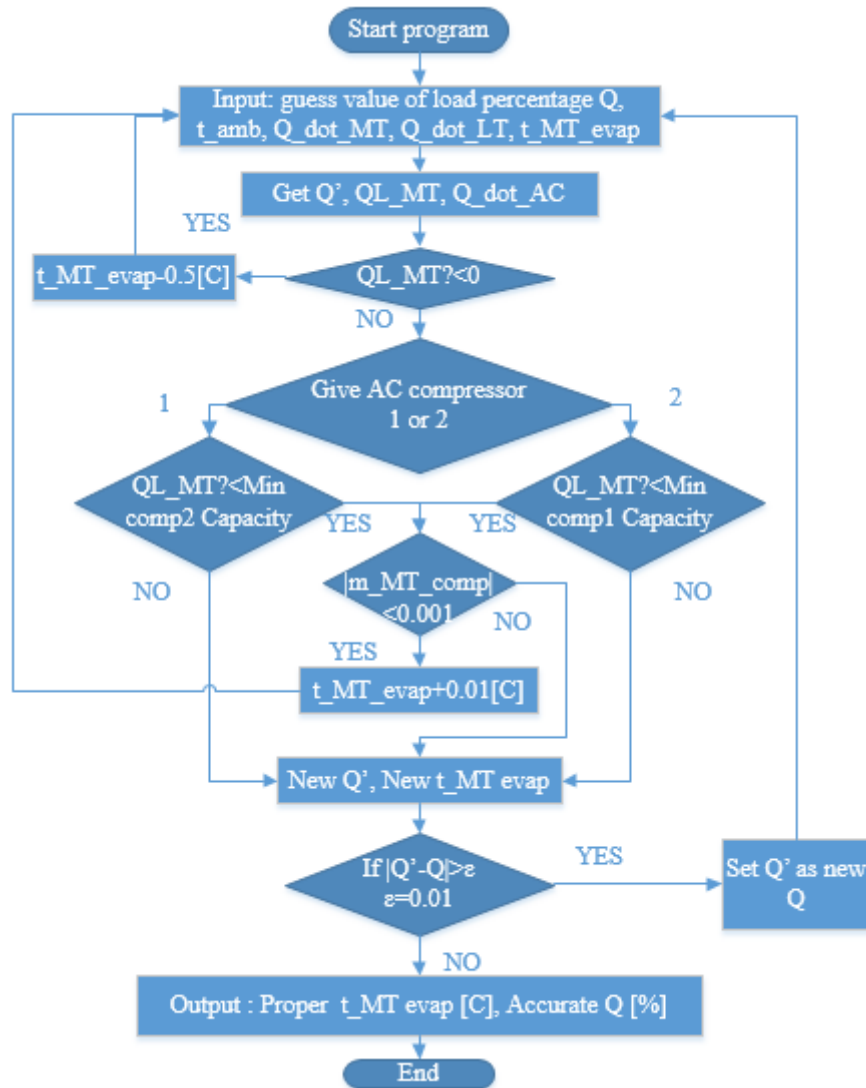
Fig. 26 Logic diagram of the system calculation

The input parameters are gas cooler load percentage Q, ambient temperature, MT cooling load, LT cooling load and MT evaporation temperature, while the outlet parameters are modified (proper) MT evaporation temperature and accurate gas cooler load percentage. The intermediate parameters acquired include mass flow rate of ejector nozzles, compressors and evaporators.

4.2.4 Results and analysis

According to the preparation above, several key parameters should be taken into consideration. For instance, the AC, MT and LT loads at same time for different ambient temperature; the pressure ratio of high side pressure over ejector diffuser pressure; the correlation of CO_2 temperature at the outlet of Gas cooler with ambient temperature; the COPs of AC, MT and LT side; how does the proper MT evaporator temperature change with ambient temperature and MT load; the difference between the new pressure level of MT evaporator and the previous one.

To investigate the system performance, a load profile including the MT cabinet, LT freezing cabinet and air conditioning system should be introduced first. Figure 27 shows the cooling load for AC, MT and LT side. This is an assumption based on maximum load of a normal supermarket as well as the minimum capacity of the chosen compressors. The ambient temperatures in the range from 25°C to 47.5°C are then chosen as input parameters. For each ambient temperature, a corresponding MT cooling load, a proportional AC cooling load and a relatively constant LT load are given.
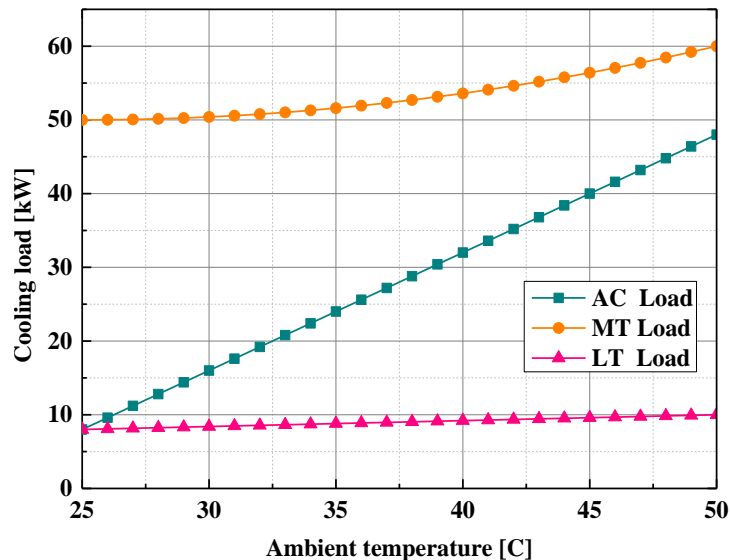
Fig. 27 Cooling load of MT, LT and AC side

To implement compressor information in the simulation work, the allocation plan associated with cooling load of each side should be specified. As the maximum load of one side is lower than 60 kW, the compressor 4 is actually not applied unless if the MT capacity is increased over 100 kW. This could occur if the supermarket is refurbished and some cabinets are changed to a much larger size in the system, when a lot of cooling load is required by a large batch of warm food, or with long periods of goods' refilling, when plenty of heat infiltrates the cabinets.

The allocation plan for the MT and AC compressors with assumed cooling loads according to different ambient temperatures, and the corresponding rotation speeds of these compressors are listed in table 7. As is seen in the table, when AC load starts to rise, compressor 1 is used for AC and compressor 2 & 3 are used for MT, as AC is able to carry more load from MT side, compressor 3 is shut down on MT and the revolution of compressor 2 is turned up to 1854 rpm from 973 rpm. When AC load rises up to 19.2 kW, higher than the minimum capacity of compressor 1, if compressor 1 and 2 are switched to the other side a gap that cannot be covered here exist, which requests compressor 1 to work at a frequency of 87 Hz or 12 Hz; but if compressor 1 on AC side is allowed to work at a frequency higher than 60 Hz, then both compressors can work with proper frequencies. Compressor 3 and 1 are then shut down when ejector takes all load from MT side and compressor 3 is added when compressor 1 is not large enough

to cover all air conditioning load till it reaches to 40 kW.

Table 7 Allocation strategy for MT and AC side

QL_AC [kW]	QL_MT [kW]	Comp 1 share [kW]	Comp 1 rpm	Comp 2 share [kW]	Comp 2 rpm	Comp 3 share [kW]	Comp 3 rpm
8.00	45.66	8.00	778	27.51	1700	18.15	1842
9.60	43.32	9.60	933	25.17	1556	18.15	1842
11.20	40.57	11.20	1089	22.42	1386	18.15	1842
12.80	37.43	12.80	1244	19.28	1192	18.15	1842
14.40	33.90	14.40	1400	15.75	973	18.15	1842
16.00	29.99	16.00	1555	29.99	1854	0.00	0
17.60	25.70	17.60	1711	25.70	1589	0.00	0
19.20	21.00	19.20	1866	21.00	1298	0.00	0
20.80	15.95	15.95	1912	20.80	1042	0.00	0
22.40	10.51	10.51	1260	22.40	1122	0.00	0
24-36.8	0.1-0	0.00	0	24-36.77	1202-1841	0.00	0
38.40	0	0.00	0	16.01	802	22.39	1842
40.00	0	0.00	0	17.61	882	22.39	1842
41.60	0	0.00	0	19.21	962	22.39	1842

	MT		AC

Except for the allocation plan, the real compressor efficiency, affected by the rotation speed of the motor of the compressor, should also be specified. The real compressor efficiency can be expressed in equation 4.3.

$$\eta_r = \eta_f \cdot \eta_{overall} \tag{4.3}$$

Where η_r represents the real compressor efficiency and η_f represents the efficiency with varied frequency (frequency efficiency). This efficiency is fitted with the compressor efficiency data with a suction pressure of 40 bar, which will be shown in chapter 5. Though the frequency efficiency is not necessarily the same for the compressors, it is assumed the same as that of the SINTEF 100 kW compressor, ignoring the difference and making it possible to calculate. It is fitted to a polynomial equation 4.4 and the coefficients are listed in table 8, where "r" represents for the compressor rotational speed in rpm. A curve depicting this efficiency is given in figure 28. The frequency efficiency reaches to 1 with a revolution of 1500 rpm and falls down when the revolution gets lower or higher.

$$\eta_f = a_0 + a_1 r + a_2 r^2 + a_3 r^3 \tag{4.4}$$

Table 8 Polynomial coefficients of the frequency efficiency polynomial

Coefficient	a_0	a_1	a_2	a_3
Value	5.35E+01	4.28E-02	-2.30E-05	3.94E-09
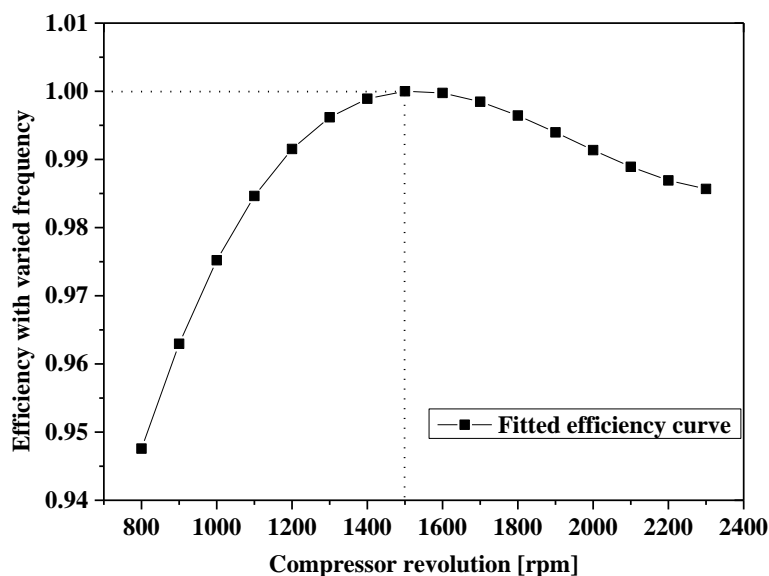
Fig. 28 Frequency efficiency as a function of the compressor rotational speed

When frequency efficiency is applied in the simulation code, the pressure ratio of MT and AC side in different ambient temperatures can be illustrated in figure 29. The LT pressure ratio is not presented for it does not change over ambient conditions. As is seen in the diagram, the pressure ratio at the MT side increases slowly in the ambient temperature range from 25 to 40 ℃ , and grows even faster after 40 °C. However, because of the upper limit of high side pressure 120 bar and the set limit of evaporation temperature 4.8°C of AC side, the pressure ratio of the AC side remains constant when the ambient temperature is larger than 40 °C.
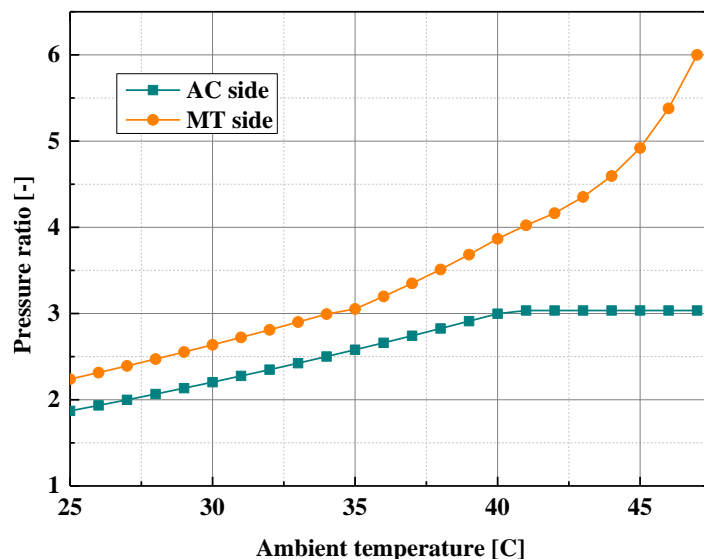
Fig. 29 Pressure ratio of MT, LT and AC side as a function of the ambient temperature

In the meantime, the gas cooler load, which is set to 1 initially as an input parameter for calculation, is acquired in the same ambient temperature range. The outlet

temperatures of the gas cooler are obtained subsequently. Both parameters are intermediate parameters, which are results of one try and the beginning parameter of the next. The gas cooler outlet temperature is used to define the inlet stream enthalpy of the ejector motive nozzle, and then taken into the energy conservation equations in ejector mixing chamber. In fact, two significant parameters in this program are coupled and need to be confirmed by recalculation. One is the real gas cooler load percentage, the other is the MT evaporator temperature. The two critical parameters are calculated and illustrated in figure 30 and figure 31.

The correlation between gas cooler load and outlet temperature has been given in equation 4.2. As is seen in figure 30, due to the large AC and MT load at high ambient temperature, the increasing rate of the real gas cooler load climbs as the ambient temperature increases, while the gas cooler outlet temperature increases more proportionally with the ambient temperature.

The proper MT evaporation temperature is adjusted according to the MT and AC load. When MT and AC load both are lower than the minimum capacity of the smallest compressor, all compressors are shut down and the bypass valve is used to lift the pressure from LT reservoir to the MT separator. If the MT load is within the adjustable capacity range of the smallest compressor, then compressor 1 is allocated for MT and compressor 2, 3 and 4 are given to AC side. When AC load reaches up to a higher value where the ejector takes most or all load of MT compressor, the MT side is shut down completely and all compressors are given for AC side. The capacity of the smallest compressor shut down in MT side would then result in a rebalance of mass flow at each point of the model system, seen in the little bulge in figure 31. Due to the rebalance of mass flow, the MT evaporation temperature is lifted a bit up by 1°C.

After the bulge, as ambient temperature increases continuously, the MT evaporation temperature gets down gradually. Because ejector takes more refrigerant at suction nozzle and the extra power generated from suction nozzle makes pressure (temperature) lift from MT evaporator to AC evaporator larger, but AC evaporation temperature is fixed to 4.8°C. Therefore the MT evaporation temperature gets lower.

On the contrary, if the ambient temperature declined down to a lower value where ejector is not able to take all load from MT side, compressor 1 is reinstalled in MT side, and the MT evaporation temperature would undergo a small dip and then goes up to - 2 °C.
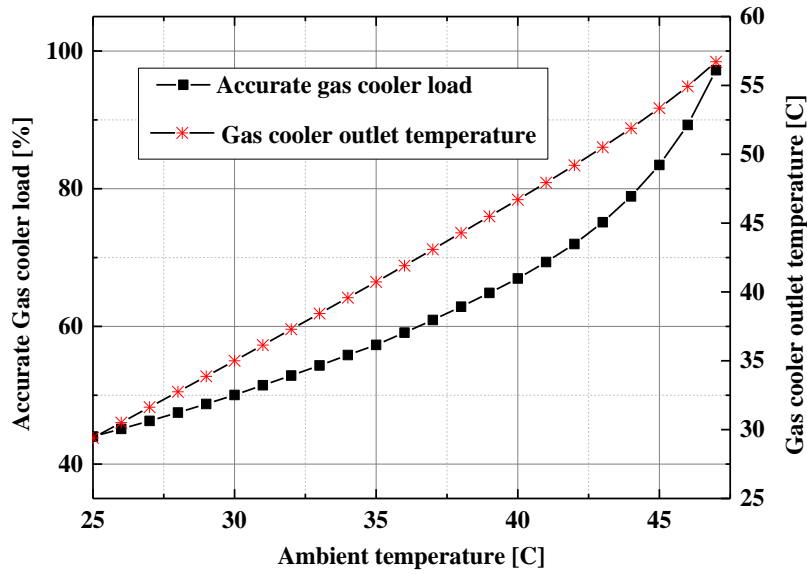
Fig. 30 Gas cooler load and outlet temperature as a function of the ambient temperature
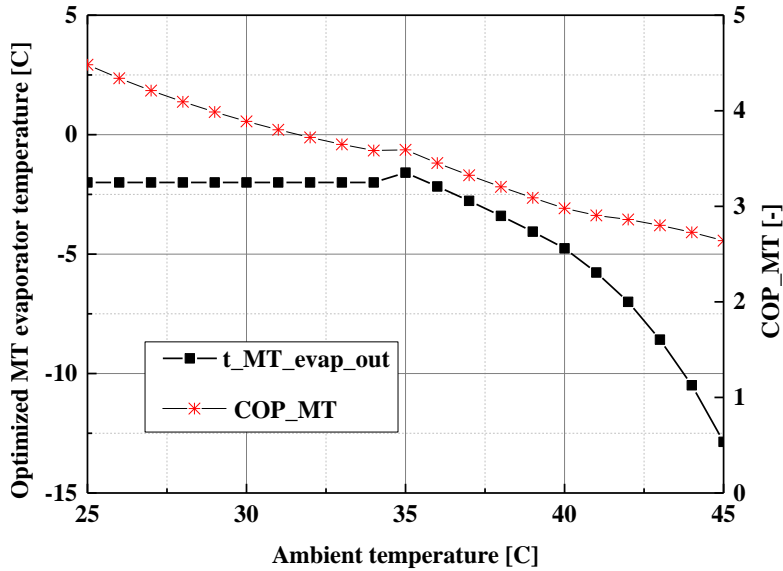
Fig. 31 Optimum MT evaporator temperature and the COP of MT side as a function of ambient temperature

Finally the COP of each side is illustrated with ambient temperature range from 25 to 46 ℃ in figure 32. COP of MT is the evaporator cooling capacity over the sum of the power consumption of MT compressor, the ejector suction nozzle enthalpy difference and the power consumption of AC compressor caused by suction flow in ejector.

It is shown that for ambient temperatures lower than 31°C, COP of MT side is higher than 4.5, and that of MT and LT side is higher than 3.8 and 1.9, respectively. COPs of each side decline as ambient temperature increases generally. However, the COP of LT side remains rather constant throughout the range, while COP of MT and AC side descend distinctly. The COP of AC, MT and LT side at the highest ambient temperature 46°C are 3.3, 2.4 and 1.7, respectively.
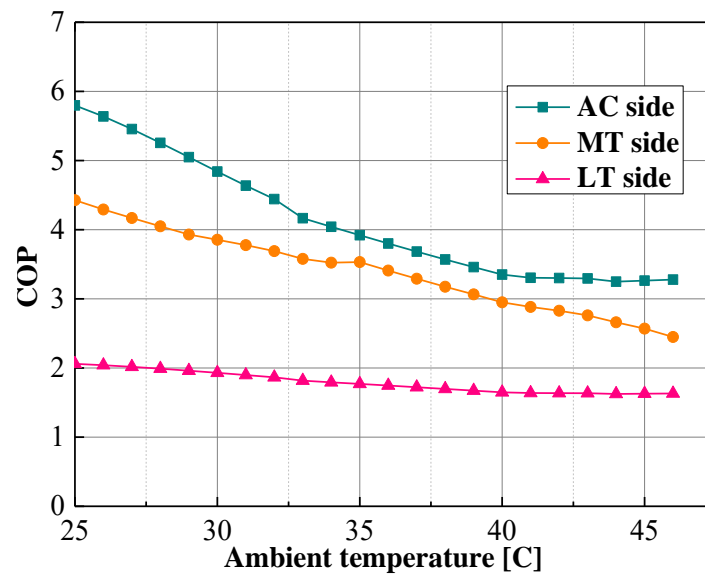
Fig. 32 COP of each side

4.3 Conclusions

In this chapter a simple case and a comprehensive case, where a numerical model is build up, are calculated and analyzed to show the coefficient of performance of MT, LT and AC parts, and how do different intermediate parameters change with the variation of the ambient temperature. The intermediate parameters including MT evaporation temperature and gas cooler load are also given along different ambient temperatures as supplement. Several conclusions can be acquired from the simulation results as follow:

1. In the simple case where only one compressor is allocated for each side, each operation condition has a corresponding balance point. As the ejector removes more vapor from the LT accumulator which results in lower evaporation temperatures, even without the MT compressors in operation. Thus the MT side can work properly either if the ejector efficiency is set to a low value or if the efficiency can be adjusted in case that 100% ejector suction vapor from MT side (MT compressor shut down).

2. Each ambient temperature has a corresponding optimized operation high side pressure. The COP changing range reflects that ambient temperature has great influence on it. This means that when high side pressure is lower, the COP of MT loop is more sensitive to the temperature change. The optimum high side pressure is applied both in the simple case and in the realistic case.

3. In the load calculation part, it is proven that 4 compressors with 2 converters can fully cover all the load gaps from 7 to 100 kW, if only the MT side is considered. However, if MT and AC are both considered and AC is prioritized, the smallest gap that exists in the MT side is 3.24 kW and the largest gap is 15.93 kW. The gaps that cannot be covered are calculated with compressor working at compressor rotational frequencies either lower than 30 Hz or higher than 65 Hz.

4. COP of MT, AC and LT side are estimated to be 2.4, 3.3, 1.7 respectively at an ambient temperature of 46 °C. The result is acquired with frequency efficiency, real gas cooler load percentage, and the proper MT evaporation temperature applied.

5. Compressor test rig and experimental results

Carbon dioxide (R744) was reintroduced as a working fluid by Lorentzen et al. [27-29] (1992/1994/1995). Many advantages of this natural substance are realized in various mobile and stationary applications ranging from heat pumps, air conditioning to refrigeration. The developed and built R744 test facilities for compressors and heat exchangers in the 100 kW to 400 kW cooling capacity range improved drastically during the last 20 years. However, there is still a massive need for further investigation to improve the efficiencies of compressors at different frequencies and on part load scenarios.

The test plant analyzed in this section was built in order to conduct experiments on high capacity components like compressors, heat exchangers, expansion and work recovery devices in a real refrigeration cycle using R744 as refrigerant. The maximum electric power input to the compressor is 100 kW, and the plant is able to work in real system performance from evaporation temperatures around triple point of R744 to maximum discharge temperature of 130 bar. Besides a closed system using R744, it has an additional supporting system using ethylene-glycol-water to reject and recover heat from the R744 system. The plant is developed by SINTEF in cooperation with Obrist engineering where it was built, and eventually installed in the laboratories of SINTEF and NTNU in Trondheim.

In this thesis work, several critical parameters of compressor performance including oil circulation ratio, volumetric efficiency and overall efficiency under different revolutions and pressure ratios are tested. A correlation of efficiency with compressor frequency is fitted also with the test points obtained at suction pressure 40 bar. This correlation is used in the simulation work where the swept volume is adapted and the revolution range is relatively fixed. All the efficiency data are further adopted to substitute one or more compressors in the previous simulation work and to try whether 2 compressors can cover as much load as possible. The system with data of this compressor can serve as a reference system and compared to the previous comprehensive model to get a comparison of annual energy consumption, which would specify whether it is possible to adopt high capacity compressor and how much energy would the better plan save.

5.1 Description of the test facility

Figure 33 shows the container where the rig is implemented. Along with a water cooled heat exchanger the air cooler is rejecting the heat applied by the compressor to the refrigerant which cannot be conserved in the supporting glycol-water system.

Fig. 33 View from the outside of the container
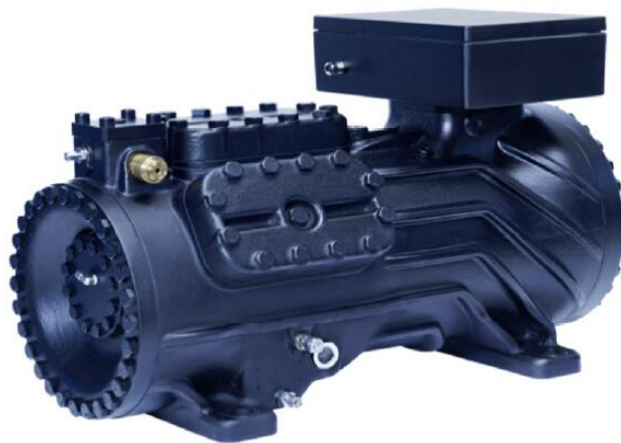
Fig. 34 Sintef R744 compressor[30]

The rig is built as flexible as possible, and all the key components in the R744 refrigerant circuit are replaceable or additional equipment as expansion or work recovery devices can be installed in parallelfor future experiments. The system is set to work at a maximum discharge pressure at 130 bar with temperatures in ranges from -50 to 180 °C in the R744 cycle and the maximum electrical power input to the compressor is close to 100 kW. For safety reasons the rig was controlled by a 3rd party company specialized in quality assurances of welding using x-ray. It has been pressurized up to 160 bar and leakage tested.

The main philosophy behind the design of the test facility is to get a flexible device which allows the investigation of different components alignments such as parallel and serial heat exchanger configurations. A sufficient amount of high accuracy measurement devices enables a detailed study of heat exchanger performance and compressor efficiencies.

The main improvements and efforts made in this compressor development are related to the following key points: thorough oil separation inside the electric motor on the suction side of the compressor; good integration of a permanent magnet motor; smart

heat management of the compressor, advanced valve design to be able to operate at a large rpm range; improved cylinder sealing concept to reduce blow by and sophisticated internal pressure equalization concept.

In general the rig consists of two independent closed systems, one using R744 as refrigerant getting compressed in the gas phase, and cooled either in critical or sub-critical conditions. As a supporting system the ethylene system worked both as heat sink and heat source at constant temperature. In certain experiments that focus on the compressor it is not required to use the supporting systems, and the ethylene water systems are not in operation during the test.

Shown in figure 35 is the schematic circuit layout (P&ID) of the test facility. A frequency converter controls the rotational speed of the compressor (1). The refrigerant conditions on the inlet and discharge side of the compressor are monitored and measured with dedicated pressure and temperature sensors. During a test campaign a special designed cylinder head plate can be installed, which allows to do pressure indication inside the cylinder. The efficiency of the frequency converter is calibrated, i.e. the electrical power input to the compressor may be measured upstream of the frequency converter. The refrigerant mass flow rate is measured upstream of the compressor suction port with a Coriolis mass flow meter (13).
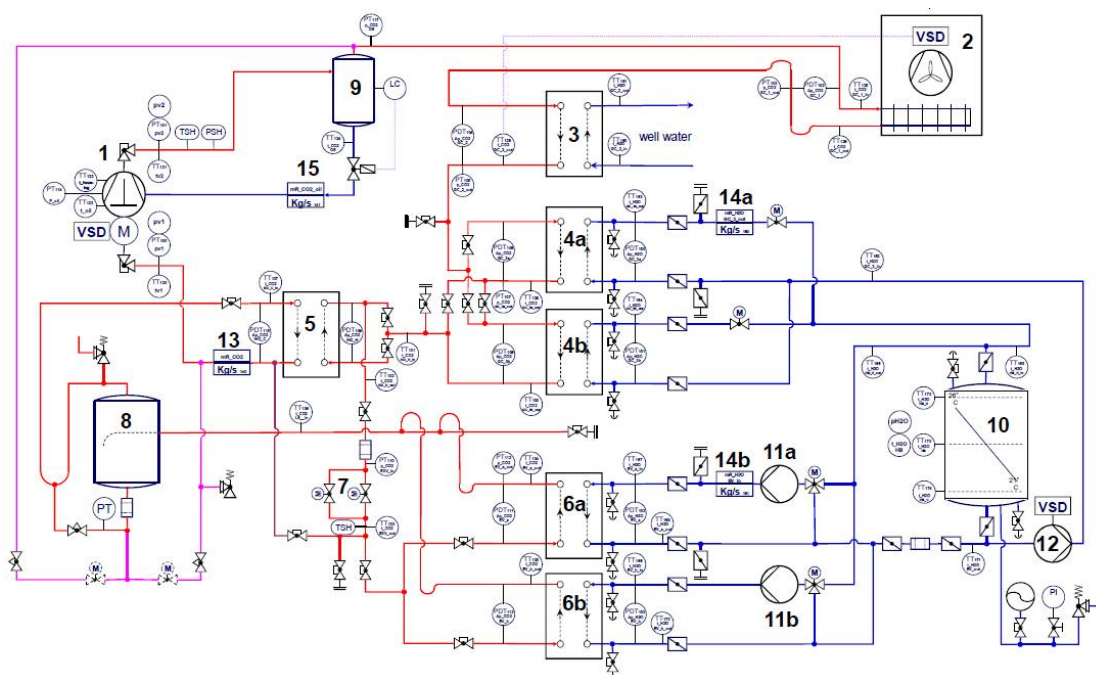

Fig. 35 Schematic circuit of the test facility. The main components are: 1) R744 compressor, 2) air cooled gas cooler, 3) water cooled gas cooler, 4a) and 4b) gas coolers/condensers, 5) internal heat exchanger, 6a) and 6b) evaporators, 7) expansion valves, 8) separator, 9) oil separator

The compressed refrigerant enters the oil separator (9) where most of the lubricant dragged is accumulated and the lubricant flow returning to the compressor crank case is measured by a Coriolis mass flow meter (15). Thereafter the refrigerant flow enters the external cooling device (2). The gas cooler/condenser is able to reject the entire heat from the compressor power input to the ambient air. In case of an indoor installation of the entire test facility the refrigerant to liquid plate heat exchanger (3) is applied to reject the surplus heat to an external heat sink.

The temperature of the refrigerant flow rate is further reduced in the gas coolers/condensers (4a&b). Depending on the operating conditions these two heat exchangers can either be arranged in series or in parallel. The absolute pressure level is measured at the outlet port of each heat exchanger, as well as the pressure drop on both sides of the plate heat exchangers.

Downstream of the gas coolers an internal heat exchanger (5) is installed, able to exchange heat from the refrigerant flow upstream of the expansion devices (7) and the downstream flow of the low pressure receiver (8). The pressure drop across the internal heat exchangers is measured as well as the exit temperatures of the refrigerant flow. It is possible to bypass the entire internal heat exchanger on the high pressure side.

Two expansion devices (7) are installed which cover the wide operation range of the compressor. Depending on the refrigerant mass flow rates and required capacities, either one or both evaporators (6a&b) are in operation. The low pressure receiver (8) accumulates the major charge of the system and separates the liquid out of the refrigerant flow downstream of the evaporators. A certain amount of liquid refrigerant including lubricant is entering the suction line upstream of the internal heat exchanger.

The plate heat exchangers (4a&b) are connected to the evaporators (6a&b) via a glycol loop. A storage tank (10) is required to maintain stable glycol temperatures into the heat exchangers. Due to the compact glycol system a full system analysis can be performed and only the power input to the compressor has to be rejected to maintain stable operation conditions. The glycol flow rates across 4a and 6a are measured as well as the pressure drops and inlet and outlet temperatures.

If only a compressor investigation takes place the refrigerant circuit can be operated without the main heat exchangers in a gas loop only, while the compressor heat is rejected either to the ambient (2) or to a liquid heat sink (3). The entire test loop and the required control units are placed inside a 20 ft. container. It can be moved to any field test side if required. The main components are accessible via two doors, i.e. at the front end between the electrical cabinets and in the center of the side wall, close to the compressor.

For the operation mode only efficiency is tested, the system diagram can be simplified and seen in figure 36. It is seen in the simplified diagram that the glycol loop is removed to get a clear view of compressor part. To acquire accurate data of temperature, pressure

and mass flow rate, several test points are installed. The variables tested includes suction temperature T_{v1}, suction pressure P_{v1}, discharge temperature T_{v2}, discharge pressure P_{v2}, compressor oil mass flow rate $\dot{m}_o$, refrigerant mass flow rate $\dot{m}_m$, compressor frequency n and electrical power P_{elect}. Besides, the density of the suction gas ρ_1, the enthalpy of suction gas h_{v1} and isentropic enthalpy of discharge gas $h_{v2,is}$ are acquired from REFPROP software with suction temperature T_{v1}, suction pressure P_{v1}, discharge temperature T_{v2} and discharge pressure P_{v2}.
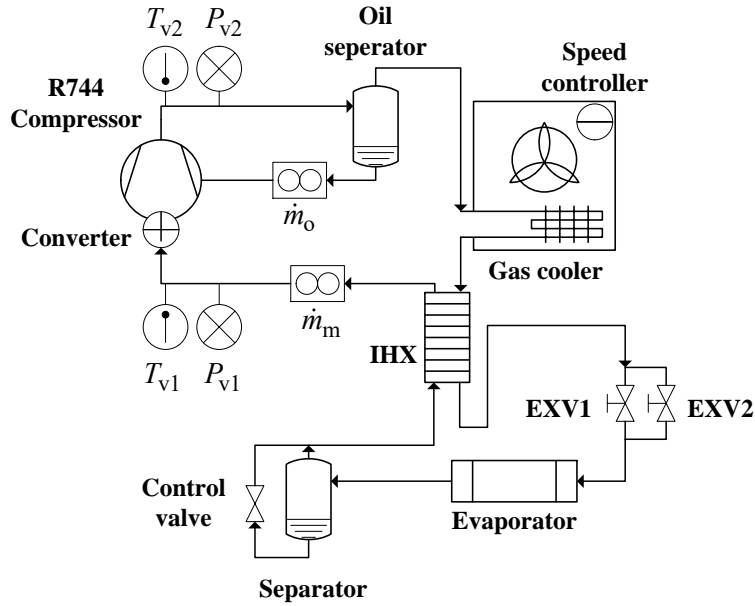
Fig. 36 Simplified overview of the experimental R744 compressor test system

The test of compressor efficiencies was conducted along the refrigeration cycle 1 to 7 as shown in figure 37. The gas conditions are at low pressure and low temperature at point 1. It is compressed from point 1 to the discharge at point 2. The compressed gas is cooled then in an air gas coolers until it reaches a point 3 where the heat from the compression is removed and no longer in the system. It is superheated to a point 1 at the inlet of the compressor in the end.
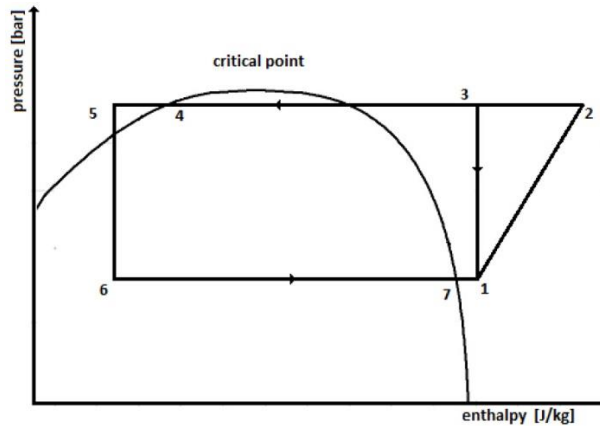
Fig. 37 Drawing of the refrigeration cycles in log p-h chart

In the cycles running to evaluate the compressor the gas the fluid was throttled from point 3 at high pressure to suction pressure at point 1. Bypassing the heat exchangers working with glycol/water mixture and using only the air cooler to remove heat generated in the compression stage.

Table 9 and table 10 summarize the compressor data and the measurement devices used in the test rig and the corresponding range and accuracy.

Table 9 Applied measurement devices

Sensors	Measured variable	Measuring device	Calibration range	Calibrated accuracy
14	Temperature (°C)	K-type thermocouple	-40-145	0.5
18	Temperature (°C)	PT100 Resistance thermometer	0-140	0.03
13	Pressure (Bar)	Pressure gauge	0-160	1.2
11	Pressure (Bar)	Pressure gauge	0-80	0.7
1	Refrigerant mass flow rate (kg/s)	Coriolis mass flow meter	0.0-1.4	0.1%
1	Lubricating oil (m³/h)	Coriolis mass flow meter	0-4	0.25%
1	Power consumption (kW)	Digital wattmeter	0-100	0.5%
1	Compressor revolution speed (rpm)	Analog signal from the inverter	0-4000	1.3%

Table 10 Main compressor data

Compressor data	Value/Range
Height*Width*Length [mm]	500*440*830
Weight [kg]	286
Volume flow rate [m^3/h]	18-90
Displacement [cm^3]	380
Max power consumption [kW]	100
Revolutions per minute [rpm]	800-4000
Frequency range [Hz]	53-267

5.2 Experimental set up and results

To describe the compressor working condition, the pressure ratio, the isentropic enthalpy difference between inlet and outlet, the volumetric efficiency, the overall efficiency and the oil circulation ratio are defined in equation 5.1 to 5.5. Equation 5.1 represents the pressure ratio, expressed as discharge pressure over suction pressure.

$$\pi = \frac{P_{v2}}{P_{v1}} \tag{5.1}$$

$$\Delta h_{is} = h_{v2,is} - h_{v1} \tag{5.2}$$

The overall efficiency is defined as shown in equation 5.3. The total mass flow rate is the sum of the refrigerant + lubricant mass flow rate. The isentropic enthalpy difference is calculated as the difference of the isentropic enthalpy at the discharge pressure (entropy of the compressor inlet) minus enthalpy at compressor inlet. The electric power consumption is measured, while the losses inside the frequency converter are neglected.

$$\eta_{\text{overall}} = \frac{P_{\text{is}}}{P_{\text{elect}}} \times 100\% = \frac{\dot{m}_{\text{total}} \cdot \Delta h_{\text{is}}}{P_{\text{elect}}} \times 100\% \qquad (5.3)$$

The volumetric efficiency is defined as shown in equation 5.4. The density is calculated based on temperature and pressure measurement at the suction side of the compressor.

$$\eta_{\text{vol}} = \frac{\dot{m}_{\text{total}}}{\dot{m}_{\text{theoretical}}} \times 100\% = \frac{\dot{m}_{\text{total}}}{\rho_{\text{l}} \cdot V_{\text{H}} \cdot n} \times 100\% \qquad (5.4)$$

The oil circulation ratio is defined in equation 5.5. This fraction is expressed as the mass flow rate of refrigerant over the sum of the total mass flow.

$$OCR = \frac{\dot{m}_{\text{o}}}{\dot{m}_{\text{total}}} = \frac{\dot{m}_{\text{o}}}{\dot{m}_{\text{o}} + \dot{m}_{\text{m}}} \qquad (5.5)$$

The measured signals from the different transducers of the test facility are connected to data sampling modules which deliver the signals to the data acquisition tool (LabVIEW). When steady state conditions are obtained the measured data are exported to an MS Excel based calculation sheet to further convert the measured data to useful results, i.e. efficiencies, performance data, etc.

Experimental results obtained at 1500 rpm at a discharge pressure of 85 bar and a 10 K superheat at the compressor inlet are shown in Figure 38 for an overview of efficiency comparison. As a reference measured values of two different R744 compressors from renowned manufactures are also implemented in the figure. The benchmark compressors were off-the-shelf, however, their displacement was only around 33% compared to the newly developed 6-cylinder unit.
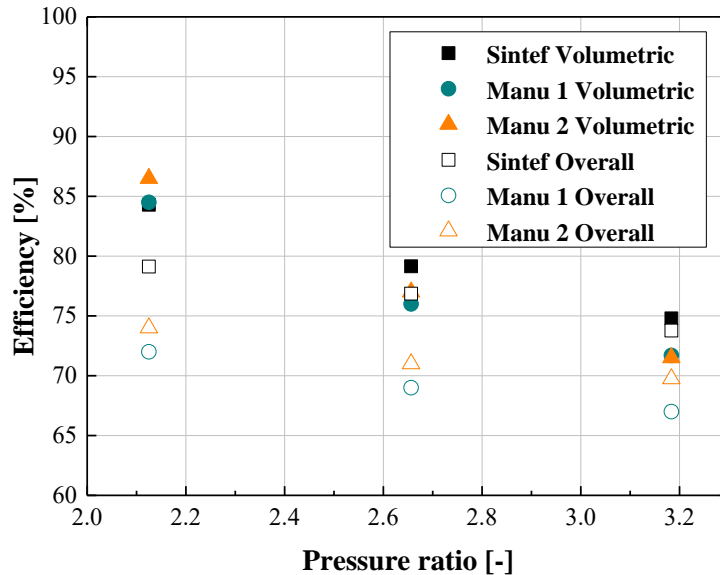

Fig. 38 Measured volumetric and overall efficiencies of R744 compressors as a function of the pressure ration. Comparison with data from off-the-shelf compressors of 2 manufacturers

Several test conditions are experimentally investigated then with different discharge

pressures, suction pressures and compressor revolutions, which are listed in table 11. Additionally, the superheat at compressor suction side is set to 10 K. The test results, including volumetric efficiency and overall efficiency are illustrated. It is clear that suction pressure and discharge pressure both have great influence on efficiency, while compressor revolution has not much impact. Nevertheless, the efficiency with varied frequency or revolution is significant in energy consumption of the system simulated.

Table 11 Test points

Condition Format: Suction pressure [bar]-Discharge pressure [bar]-Revolution [rpm]		
40-85-1000	40-80-1000	40-75-1000
40-85-1500	40-80-1500	40-75-1500
40-85-2000	40-80-2000	40-75-2000
40-85-2500	40-80-2500	40-75-2500
32-85-1500	32-80-1500	32-75-1500
32-85-2000	32-80-2000	32-75-2000
32-85-2500	32-80-2500	32-75-2500
27-85-1500	27-80-1500	27-75-1500
27-85-2000	27-80-2000	27-75-2000
27-85-2500	27-80-2500	27-75-2500

The compressor efficiency and oil circulation ratio with suction pressure 40 bar and discharge pressure 80 bar are shown in figure 39 as a function of the rotational speed of the compressor. The test results for single parameter, i.e. volumetric efficiency are shown afterward.
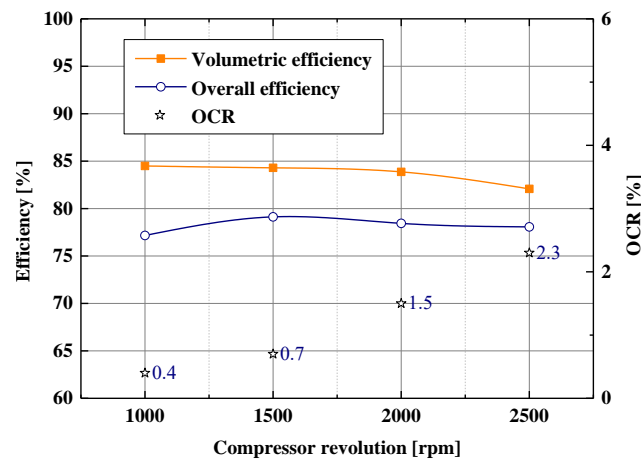
Fig. 39 Efficiencies and oil circulation ratio vs. revolution with suction pressure 40 bar and discharge pressure 80 bar as a function of the compressor rotational speed

5.2.1 Oil circulation ratio

The oil circulation ratio at all test points is illustrated in figure 40. Oil circulation ratio is one of the most important parameters that affect compressor performance. A too high ratio would lower down the performance of the heat exchanger, while a too low ratio may results in insufficient lubrication and reduce the compressor efficiency.

As is seen in figure 40, the oil circulation ratio is higher than 0.6% when the rotational speed is higher than 1500 rpm. On the one hand, high rotational speed enlarges the pressure drop, which causes friction loss and more oil consumption. Therefore the oil circulation ratio rises. For instance, the oil circulation ratio at a pressure ratio of 2.0 and a rotational speed of 2500 rpm is about 70 times of that at 1000 rpm. On the other hand, as pressure ratio lifts, the higher pressure drop decides more oil consumption. Nevertheless, the flow rate descends with a lower pressure ratio, resulting in less oil consumption. Thus, the oil circulation ratio increases at first as the pressure ratio lifts and decreases then as the pressure ratio rises to higher values. The maximum oil circulation ratios are acquired in the pressure ratio range from 2.0 to 2.1. For instance, the highest circulation ratio is obtained at a pressure ratio of 2.1 and rotational speed of 2500 rpm. Thus the area at line 2500 rpm and between pressure ratio lines 2.0 to 2.2 is an optimum region in figure 40, due to the benefit for lubrication. However, this "optimum" region is decided according to specific external conditions, because too high circulation ratio is not suitable for systems that requires better heat exchanger performance.
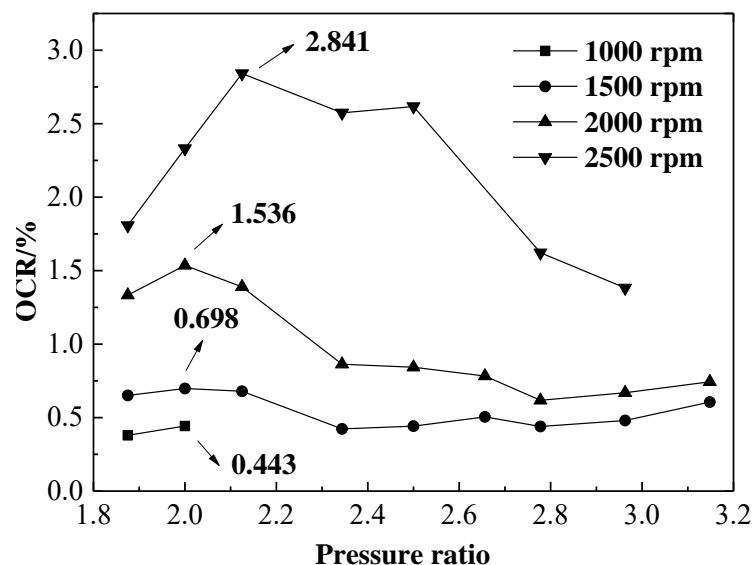
Fig. 40 Oil circulation rate as a function of pressure ratio and rotational speed of compressor

5.2.2 Volumetric efficiency

Volumetric efficiency is a critical parameter describing the discharging performance of a compressor. Previous volumetric efficiency data (in different suction pressure and discharge pressure) are illustrated in figure 41 as a function of pressure ratio, as pressure ratio is a more frequently used parameter for efficiency evaluation. For the reason that larger pressure ratio decides a lower gas transmission coefficient, the volumetric efficiency decreases clearly as pressure ratio rises. For instance, the volumetric efficiency declined by 11% from pressure ratio 1.88 to 3.2 at a rotational speed of 2500 rpm.

Fig. 41 Volumetric efficiency as a function of pressure ratio and rotational speed of compressor

If kept constant the pressure ratio, the volumetric efficiency generally descends as rotational speed rises rises, except for several exceptional points. For instance, the volumetric efficiency at rotational speed of 1000 rpm is predicted to be higher than that at 1500 rpm with pressure ratio of 2.78, while it is opposite in the result. Higher rotational speed of the compressor accelerates the gas flow where pressure drop is positively proportional with flow rate. The compressor temperature and internal leakage would therefore increase.

Overall, among all the test points, the maximum volumetric efficiency is 85.5%, acquired at a pressure ratio of 1.88 and revolution 1000 rpm.

5.2.3 Overall efficiency

In practical engineering, frequency converter is usually used to vary compressor rotational speed and to fit the requested cooling capacity. The cooling capacity and efficiency both reach a maximum at the rated rotational speed. However, this optimal rotational speed should be confirmed with massive experimental data. In this thesis, the experimental data obtained are compared with previous test results performed by Armin, et al.[30]. It turned out that the optimum revolution and pressure ratio from the two tests agree with each other well.

The correlation between overall compressor efficiency with pressure ratio and rotational speed is shown in figure 42. On the one hand, it is clear that with constant rotational speed, compressor efficiency increases as pressure ratio rises and then declines as pressure ratio exceeds 2.1. The highest overall efficiencies are acquired between the pressure ratio 2.0 and 2.1 in both tests. On the other hand, with constant pressure ratio, the optimal overall efficiency is reached at rotational speed 1500 rpm. However, when pressure ratio is larger than 2.8, the overall efficiencies at different rotational speeds converge.
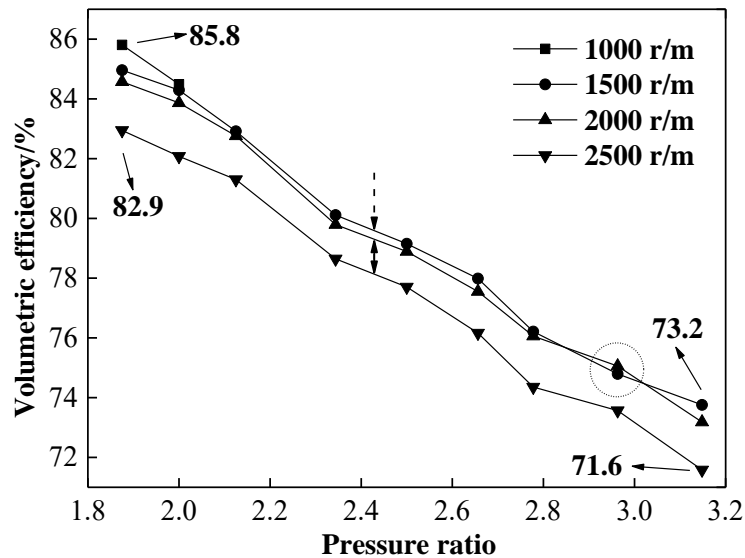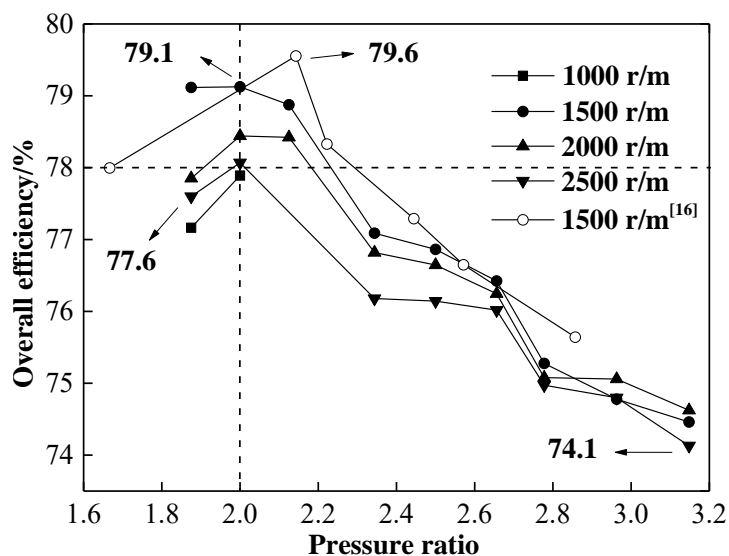
Fig. 42 Overall efficiency, as a function of pressure ratio and rotational speed of compressor

5.2.4 Comparison with specific compressor products

Upon acquiring the experimental data, a polynomial fitting for the overall efficiencies is conducted. It is used to compare with the efficiency data of two compressors from Dorin and Bitzer. This data are acquired from the database of Pack Calculation software[31]. The results are expressed both in equation 5.6 and in figure 43. The coefficients used in correlation 5.6 for the different compressors are listed in table 12.

Table 12 Polynomial coefficients and the efficiency formula of existing products

	a	b	c	d	e	R-coef.
Sintef	-9.73E-01	2.78E+00	-1.59E+00	3.94E-01	-3.61E-02	9.89E-01
Bitzer	6.20E-01	2.62E-02	-1.87E-03	-1.32E-03	1.47E-04	-
Dorin	5.71E-01	5.84E-02	-9.50E-03	1.44E-18	-7.64E-20	-

$$\eta = a + b\pi + c\pi^2 + d\pi^3 + e\pi^4 \tag{5.6}$$
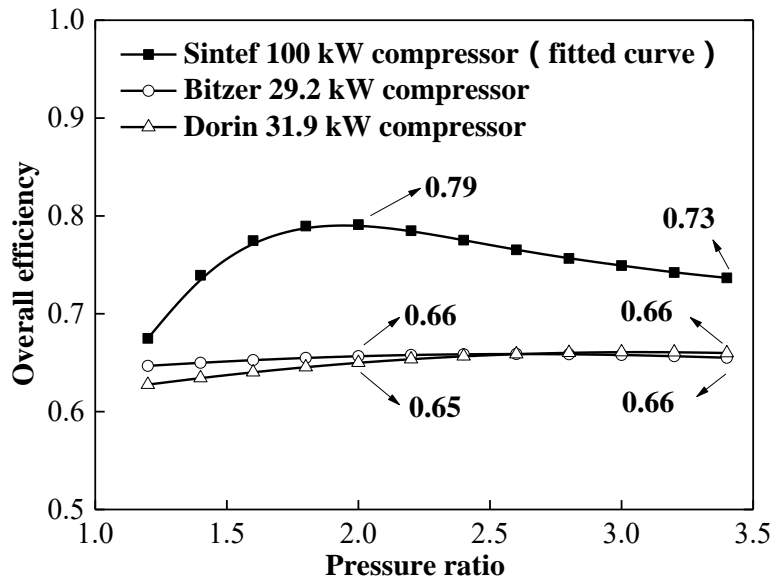
Fig. 43 Comparison of experimental data obtained in this thesis, at rotational speed 1500 rpm, with the efficiency of two off-the-shelf R744 compressors

According to figure 43, the highest overall efficiency is 0.79 obtained at a pressure ratio of 2.0 and a revolution speed of 1500 rpm, which is 17% higher than with Bitzer's compressor. An efficiency of 0.73, obtained at pressure ratio 3.2, is 11.5% higher than with Dorin's compressor. Therefore, the overall efficiency of this Sintef 100 kW compressor is much higher than that of off-the-shelf compressors of similar characteristics.

The improved performance of Sintef compressor comes from the design architecture and system installation.
The main improvements and efforts made in this compressor development are related to:
• Thorough oil separation inside the electric motor on the suction side of the compressor.
• Well integration of a permanent magnet motor.
• Smart heat management of the compressor
• Advanced valve design to be able to operate at a large rpm range.
• Improved cylinder sealing concept to reduce blow by.
• Sophisticated internal pressure equalization concept.

5.3 Discussion
The extensive measurement results indicate a significant efficiency improvement obtained with the new 6-cylinder R744 compressor developed in cooperation between SINTEF and Obrist Engineering GmbH. But a further improvement of both the overall and volumetric efficiency can be expected.

The overall efficiency is not decreasing at higher pressure ratios in the same way as it does with existing R744 piston compressor. This shows that the new concept has a large potential when applied in heat pumps, where due to large temperature lifts elevated pressure ratios are expected.

The optimum, i.e. the highest overall efficiency values with the current valve arrangement are obtained between 1000 and 2000 rpm. When analyzing load profiles of ordinary refrigeration systems as applied in commercial refrigeration 80 % of the compressor operation could take place at these conditions, i.e. a high system COP can be achieved which results in a high energy efficiency of a supermarket as an example.

This compressor concept can help the industry and the end user to achieve the next level on the way to further improve the energy efficiency of energy intensive installations which contain heat pumping equipment. High temperature heat pumps and large commercial refrigeration plants are potential applications for this high efficient compressor concept.

5.4 Comparison with 4 compressor-based pack

As described in chapter 4, the core of the simulation work is to design a logic strategy to operate a compressor rack in order to minimize energy consumption, optimize system COP, and cover the cooling load curve as smoothly as possible. A comprehensive case has been discussed subsequently with 4 compressors. Additionally, it is also indicated that the compressor efficiency experiments should be conducted to find the possibility to substitute one or two of the compressors applied in the simulation work. The model with the tested compressor serves as a reference system and it will be compared with the previous system. The COP and energy consumption will be specified for both systems with the same ambient and load conditions.

5.4.1 Effect on COP of the two strategies

When compressor 1 and the compressor tested in SINTEF/NTNU laboratory (SC compressor) are applied in the simulation, a new operation schedule can be established to cover the load defined previously, which is shown in table 13. It is clear that when the AC cooling load is less than 20.8 kW, compressor 1 is allocated for AC and SC is used for MT, and vice-versa. The isentropic efficiency as well as frequency efficiency data are also applied.

Table 13 Allocation strategy for MT and AC side (reference model)

QL_AC [kW]	QL_MT [kW]	Comp 1 capacity [kW]	Comp 1 rpm	Comp SC capacity [kW]	Comp SC rpm
8.00	45.66	8.00	778	45.66	1781
9.60	43.32	9.60	933	43.32	1695
11.20	40.57	11.20	1089	40.57	1593
12.80	37.43	12.80	1244	37.43	1478
14.40	33.90	14.40	1400	33.90	1348
16.00	29.99	16.00	1555	29.99	1204
17.60	25.70	17.60	1711	25.70	1046
19.20	21.00	19.20	1866	21.00	874

20.80	15.95	15.95	1550	20.80	866
22.40	10.51	10.51	1022	22.40	925
24-36.8	0.1-0	0.1-0	0	24-36.8	984-1455
38.40	0	0	0	38.40	1514
40.00	0	0	0	40.00	1572
41.60	0	0	0	41.60	1631
43.2	0	0	0	43.2	1690
		MT			AC

With the same calculation iterate, the COP of the two models as a function of the ambient temperature is shown in figure 44. COP decreases generally as ambient temperature increases. The highest COP of AC and LT side in the reference strategy are the same as in the original strategy, whereas the maximum COP of MT reaches about 5.1. It can be seen that when the ambient temperature is less than 32 °C, the COP of AC side and LT side in the reference system remain relatively equal to that in original system, whereas the COP of MT side is averagely 0.5 higher in the reference system than that in the original system. This is due to the higher efficiency of the SC compressor.

Besides, when ambient temperature is higher than 32°C, compressor SC is switched to AC side, resulting in a significant rise in COP of AC side in the reference system. Though it is installed on AC side, the high efficiency makes ejector able to take more MT load and therefore increases the COP of MT side. Additionally, a little increase about 0.2 of the COP of LT side in the reference system can also be found due to its definition (see equation 4.10). Since the efficiency of the AC compressor is lifted, the power consumption of AC compressor with LT fluid would decline, therefore a small rise of COP exists when SC compressor applied.

Overall, the reference system with 2 compressors substituted by the compressor SC has a relatively higher COP than the original system, due to the high efficiency of the SC compressor. However, this result is based on the operation condition of compressor SC, where it is allowed to be operated at frequencies as low as 30 Hz (as the other compressors). If the SC compressor is requested to operate all at frequency higher than 53 Hz as instructed on the user manual, MT or AC cooling loads lower than 12 kW would not be covered. Therefore either strategy is applicable but with its own limitation. The reference strategy, with 2 parallel compressors for MT and AC and one compressor for LT is a better choice for the compressor pack operation when high-efficiency compressor is allowed to operate at low capacity range. In the meantime, the original strategy, with 4 compressors installed for MT and AC and capable to cover the cooling load 8-100 kW, is a better choice when the cooling load is strictly requested to be covered smoothly.
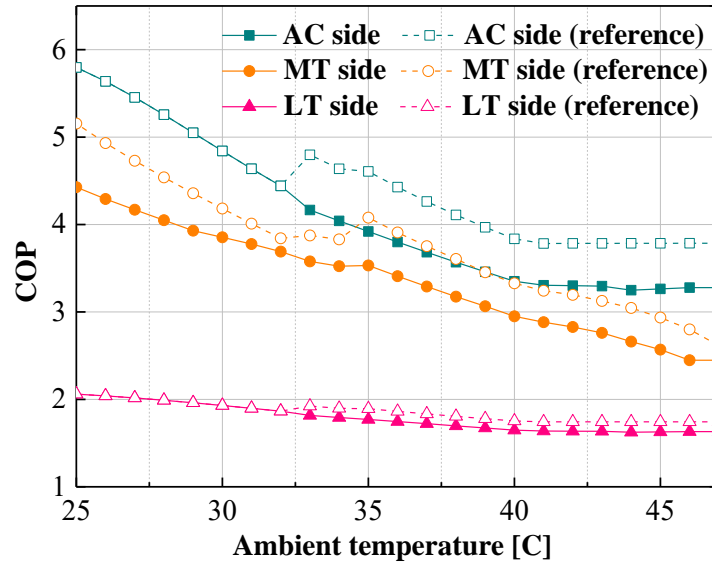
Fig. 44 AC, MT and LT COPs' comparison of the two strategies as a function of the ambient temperature

5.4.2 Comparison of energy consumption on each side

In order to analyze daily and annual energy consumption of the two strategies on each side, a daily temperature profile should be specified first. An ambient temperature curve is obtained according to the previous research performed by Y. T. Ge et al.[32], shown in figure 45. The rush hour starts from 10 a.m. and ends at 8 p.m. In this part, climate difference and season difference are assumed uniform for convenience of calculation.

Fig. 45 Daily temperature profile assumption of a typical supermarket

In order to compare the energy consumption, the SC compressor is applied in the simulation code, substituting compressors 2, 3 and 4. The reference strategy is operated with only compressor 1 and SC. The revolution range of SC is adjusted from 800 to 4000 rpm and both compressors have VSD. The mass flow rate of SC is adapted also

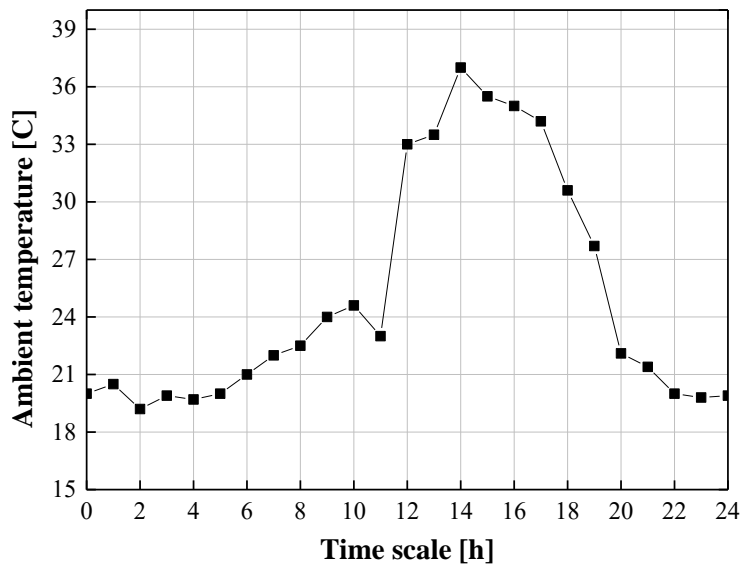in the simulation. Energy consumption is regarded as one of the most significant parameters on system strategy evaluation. In this thesis, energy consumption of each side is calculated in a scale of hours.

The power consumption of AC, MT and LT side are calculated and shown in figure 46. On the one hand, the LT side compressor power consumption is identical for both strategies (same mass flow rate and unchanged LT compressor). On the other hand, the AC side power consumption side increases faster while MT side are shut down as load rises in rush hours, because of the compressor switch. However, the power consumption of reference strategy on AC side is slightly lower than the original strategy when ambient temperature is lower, but much higher when it rises over 25 ℃ . For example, the original system consumes about 1.5 kW more than that of reference system at 8 am but about 8 kW more at 2 pm. Nevertheless, figure 46 only illustrates the energy consumption of each side of a typical day likely in summer. Different ambient conditions should be considered as well in the future.
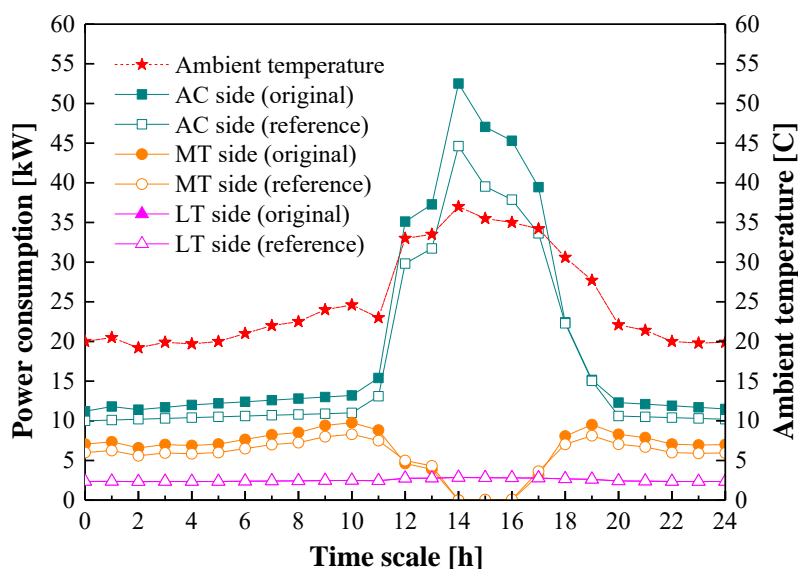
Fig. 46 Power consumption comparison on each side

5.4.3 Comparison of the two strategies on daily energy consumption

To investigate the consumption of the two strategies, the daily energy consumption of all the compressors is considered. The ambient temperature is made as input parameter and the energy consumption of both strategies are illustrated in figure 47. The shaded orange area of the figure represents the energy consumption of SC compressor based strategy (reference strategy) and the blue area represents the energy saved with SC compressors if compared to the 4 compressors based strategy (original strategy).

Fig. 47 Daily energy consumption of the two strategies

It is calculated from the simulation that the strategy with 4 compressors has a daily energy consumption of 721.7 kWh, while that for the SC compressor based system needs just 627.3 kWh per day. The reference strategy saves 13.1% power consumption of the compressor. Here the energy consumption consists only of compressors and does not consider heat compensation and internal component electricity consumption, including the electrical expansion valves, control system and other measurement devices.

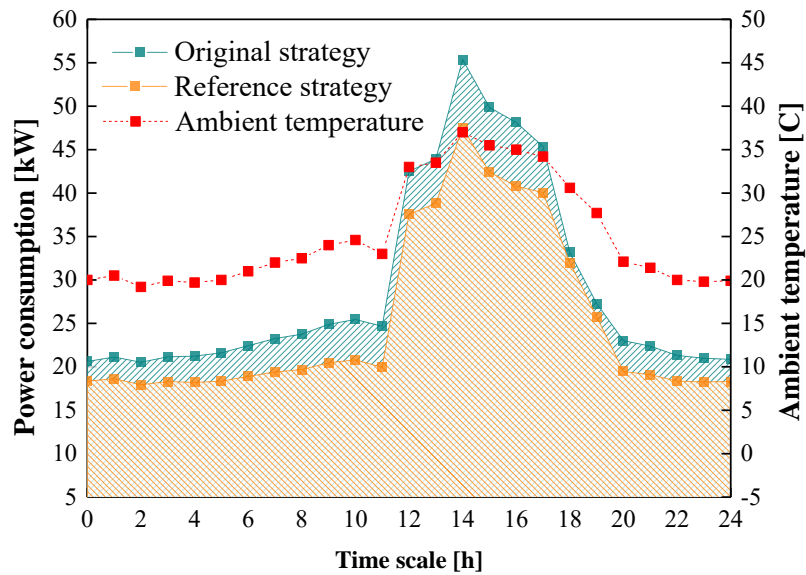## 5.5 Limitation of the simulation and experiment
The main limitations of the simulation work and experimental work are:

(1) Due to the upper limit of the high side pressure, when the ambient temperature rises towards 50 °C, the MT evaporator temperature decreases. A too low MT evaporator temperature is reached, which is unrealistic. The ejector efficiency is also necessarily set to be lower than 0.15 to make sure that not all flow are taken by ejector and that MT compressor works. Changes could be made on iterate calculation to make the simulation closer to a real case where ejector efficiency usually reaches to 0.3.

(2) The efficiency data of the selected compressors, i.e. compressor 1-4 is not precise due to the lack of data on the effect of rotation speed (frequency). These data are not available.

(3) The superheating was not accurately controlled at 10 K manual operation and stabilization, which may have impact on the experimental results.

(4) Only the energy consumption of each side of a typical day in summer is illustrated. Daily profiles for different locations and seasons should be considered as well.

5.6 Conclusions

A 100 kWel power and 400 kW cooling capacity test rig with multi-functional testing possibilities is presented. It allows measurements on R744 heat exchangers and compressors with detailed analysis possibilities. First test results are shown with test rig and the newly developed 6 cylinder R744 compressor.

The experimental results in the pressure ratio range from 1.9 to 4 and under compressor rotational speeds from 1000 to 2500 rpm are reported. The results show that the highest oil circulation rate is 2.84%, acquired with a pressure ratio of 2.1 and a rotational speed of 2500 rpm, while the volumetric efficiency reaches a maximum value 85.8% (pressure ratio 1.88 and rotational speed 1000 rpm). The optimum overall efficiencies of this compressor can be achieved in the pressure ratio range from 1.5 to 2.5 and with a compressor rotational speed close to 1500 rpm. Specifically, the maximum value is 79.1% with a rotational speed of 1500 rpm and a pressure ratio of 2.0. The fitted overall efficiency results are also compared with the efficiency data from two off-the-shelf compressors (drawn from their catalog). The overall efficiency of the new compressor is 11.5% higher than the others when pressure ratio ranges from 1.5 to 3.2.

Currently compressor racks contain several compressors to be able to maintain low and high capacities. The new concept of the wide capacity range compressor tested allows replacing several ordinary compressors with a single compressor. Therefore, the cost of installed cooling capacity is in the same range or even lower. The results indicate that the performance of the 6 cylinder R744 compressor driven by a permanent magnet motor is close to the expected efficiencies as indicated by thorough simulations. Overall efficiencies close to 80% are measured. The compressor also shows favorable efficiency at a wide range of compressor rotational speeds.

In addition, in order to minimize energy consumption and optimize system COP, as well as to meet the cooling load curve as smoothly as possible, the SC compressor tested in the last chapter is applied in the simulation work and set up as a reference strategy. The compressor efficiency is applied also and is utilized to substitute compressor 2 and 3 applied in the comprehensive simulation work. The model with the tested compressor serves as a reference strategy and is then compared with the previous system in terms of COP and energy or power consumption. According to the COP and energy consumption calculation, several conclusions are acquired as following.

(1) The reference system with compressor 1 and SC installed has a relatively higher COP on each side than the original system with 4 compressors on MT and AC side, with a premise that SC compressor is allowed to operate at frequency lower than 30 Hz.

(2) Either strategy is applicable but with its own limitation. The reference strategy is a better choice for the compressor pack operation when high-efficiency compressor is allowed to operate at low capacity range. In contrast, the original strategy is a better choice when cooling load is strictly requested to be covered smoothly.

(3) If applied an ambient temperature daily profile in summer conditions, it can be seen that the LT side compressor power consumption remains relatively constant. On the other hand, the AC side power consumption increases faster and MT side compressors are shut down as load rises in rush hours, because the largest capacity is applied to the AC side due to the strategy of prioritizing AC over MT. However, the power consumption of the reference strategy on AC side is slightly lower than that of the original strategy when ambient temperature is lower, but much higher when the ambient temperature exceeds 25℃ . For example, the original system consumes about 1.5 kW more than the reference system at 8 a.m. and about 8 kW more at 2 p.m.

(4) The strategy with 4 compressors consumes 721.7 kWh a day, while that for the compressor SC based system consumes just 627.3 kWh per day. The reference strategy saves 13.1% power consumption of the compressor. Here the energy consumption does not consider heat compensation and internal component electricity consumption, including the electrical expansion valves, control system and other measurement devices.

6 Conclusion

In this thesis, the background of reimplementation of CO_2 and a description of refrigeration cycles with R744 compressor pack and ejectors are introduced. The following are two case studies performed to set up the R744 compressor pack model and library. One is a simple model with only one compressor for each side; the other is a comprehensive model with up to 4 parallel compressors installed both for production of AC and MT cooling. The simulation work for COP analysis was conducted on both models with the necessary data from compressor databases and efficiency tests. An operation strategy for the compressor pack in the comprehensive model is also built from the simulation work. Then, a high-performance compressor available in NTNU-SINTEF laboratory (SC compressor) is tested in terms of oil circulation, volumetric efficiency and overall efficiency. The tested compressor is then applied in the simulation and an operation strategy for the reference model with only 2 compressors (including this high performance SC compressor). The operation strategies of the two models are compared in terms of COP and energy consumption.

In the simulation work of the simple case, a p-h diagram and a simplified system diagram of the cycle with 4 pressure levels are made. The COP of MT side is discussed in detail as a fundamental for the comprehensive case. It is specified that each operation condition has a corresponding balance point. If the ejector is able to transfer more vapor from the LT accumulator side towards the pressure level of the MT separator, either the pressure set point of the PA compressor should be increased or MT evaporation temperature should be reduced. Each ambient temperature has a corresponding optimized operation high side pressure. The COP of the MT circuit reaches an optimum and then falls down gradually at a fixed high side pressure as ambient temperature increases. The trend of optimum points can be marked with a line to show the system COP with certain ambient temperature and its optimum high side pressure. The correlation of this optimum hide pressure can also be applied in the comprehensive case.

In the simulation work of the comprehensive case, load calculation and operation strategy for compressors are planned. In the load calculation part, it is proven that 4 compressors with 2 converters can fully cover all the load gaps from 7-100 kW if only MT side is considered. However, if MT and AC are considered and AC is prioritised, there are gaps in the MT loads met. The smallest gap is 3.24 kW and the largest gap is 15.93 kW. The gaps that cannot be covered are calculated with compressor working at frequencies either lower than 30 Hz or higher than 65 Hz. The lowest COP of MT, AC and LT side are 2.4, 3.3, 1.7, respectively, at an ambient temperature of 46 °C.

The experimental results for the 100 kWel SC compressor, in the pressure ratio range from 1.9 to 4 and under compressor rotational speeds from 1000 to 2500 rpm, are reported. The results show that the highest oil circulation rate is 2.84%, corresponding to a pressure ratio of 2.1 and a rotational speed of 2500 rpm, while the volumetric efficiency reaches a maximum value 85.8% with pressure ratio 1.88 and rotational

speed 1000 rpm. The optimum overall efficiencies of this compressor can be achieved in the pressure ratio range from 1.5 to 2.5 and with compressor rotational speed near 1500 rpm. Specifically, the maximum value is 79.1% (rotational speed 1500 rpm and pressure ratio 2.0). The fitted overall efficiency results are also compared with the efficiency data from the catalogs of two off-the-shelf compressors. The overall efficiency of the new compressor is at least 11.5% higher than that of the others when the pressure ratio ranges from 1.5 to 3.2.

Finally, a strategy comparison between the original model (with 4 compressors on MT and AC side) and the reference model (with compressor 1 and SC compressor) is presented in terms of COP and energy consumption. Either strategy is applicable but with its own limitation. The reference system has a relatively higher COP on each side than the original system, but only if SC is allowed to operate at frequencies lower than 30 Hz and higher than 53. The original strategy is a better choice when cooling load is strictly requested to be covered smoothly.

In terms of power consumption on different sides, on the one hand, the LT side compressor power consumption remains relatively constant, independently of the ambient conditions. On the other hand, the power consumption on AC side increases faster while MT side are shut down as load rises in rush hours, because of the compressor switch. However, the power consumption of reference strategy on AC side is slightly lower than that of the original strategy when the ambient temperature is relatively low, but much higher when the ambient temperature exceeds 25°C. For example, the original system consumes about 1.5 kW more than that of reference system at 8 a.m. but about 8 kW more at 2 p.m.

The strategy with 4 compressors consumes 721.7 kWh a day, while that for the compressor SC based system consumes just 627.3 kWh per day. The reference strategy saves 13.1% power consumption of the compressor. Here the energy consumption does not consider heat compensation and internal component electricity consumption, including the electrical expansion valves, control system and other measurement devices.

7 Reference

[1] Elbel S. Experimental and Analytical Investigation of a Two-phase Ejector Used for Expansion Work Recovery in a Trans-critical R-744 Air Conditioning System[D]. Ph.D. thesis. Department of Mechanical Science and Engineering, University of Illinois at Urbana-Champaign, 2007.

[2] Robinson D., Groll E.A. Efficiencies of transcritical CO2 cycles with and without an expansion turbine[J]. International Journal of refrigeration, 1998, 21(7):577-589.

[3] Kornhauser A.A. The Use of an Ejector as a Refrigerant Expander[C]// International Refrigeration and Air Conditioning Conference. 1990: 82.

[4] Elbel S. Historical and present developments of ejector refrigeration systems with emphasis on transcritical carbon dioxide air-conditioning applications[J]. Int. J. Refrigeration, 2011, 34(7), 1545-1561.

[5] Drescher M., Hafner A., et al. Experimental Investigation of Ejector for R-744 Transcritical Systems[C]//Proceedings of the International Congress of Refrigeration (ICR), Beijing, China, 2007: ICR07-B1-742.

[6] Banasiak K., Hafner A., Andresen T. Experimental and numerical investigation of the influence of the two-phase ejector geometry on the performance of the R-744 heat pump[J]. Int. J. Refrigeration, 2012, 35: 1617-1625.

[7] Fiorenzano R. Untersuchung von Ejektor-Kaelteanlagen beim Einsatz in tropischen Gebieten[D]. Ph.D. thesis. Technische Universitaet Braunschweig, Germany, 2011.

[8] Lucas C., Koehler J. Experimental investigation of the COP improvement of a refrigeration cycle by use of an ejector[J]. Int. J. Refrigeration 2012, 35, 1595-1603.

[9] Gernemann A. Konzeption, Aufbau und energetische Bewertung einer zweistufigen CO2-Kae lteanlage zur Kaeltebereitstellung in gewerblichen Normal- und Tiefkuehlanlagen (Supermarkt)[D]. Ph.D. thesis. Universitaet Duisburg Essen, Germany, 2003.

[10] Kruse H., Schiesaro P. Entwicklung einer transkritischen zweistufigen Supermarktkae lteanlage fuer Tief- und Normalkue hlung[C]//Proceedings of the DKV-Tagung, Magdeburg, Germany, 2002.

[11] Froeschle M. Aktuelle Moeglichkeiten und Potenzial von Kae lteanlagenschaltungen mit dem Kaeltemittel R-744 (CO2)[C]//Proceedings of the DKV-Tagung, Berlin, Germany, 2009.

[12] Sawalha S. Carbon Dioxide in Supermarket Refrigeration[D]. Ph.D. thesis. KTH, Stockholm, Sweden, 2008.

[13] Girotto S., Minetto S., Neksa P. Commercial refrigeration system using CO2 as the refrigerant[J]. International Journal of Refrigeration, 2004, 27, 717–723.

[14] Sharma V., Fricke B., et al. Comparative analysis of various CO2 configurations in supermarket refrigeration systems[J]. International Journal of Refrigeration, 2014, 46, 86-99.

[15] Hafner A, et al. Multi-ejector concept for R-744 supermarket refrigeration[J].

International Journal of Refrigeration, 2014, 43, 1-13.

[16] Wiedenmann E., Schönenberger J., et al. Effiziente Kälteerzeugung im Supermarkt mittels CO2-Booster-Kälteanlage und Ejektor[C]//Deutscher Kälte- und Klimatechnischer Verein e.V. Düsseldorf: AA, 2014.

[17] Hafner A., Hemmingsen A.K., et al. R744 refrigeration system configurations for supermarkets in warm climates[C]//3rd IIR International Conference on Sustainability and the Cold Chain, London, UK, 2014.

[18] Finck O., Schrey R., Wozny M. Energy and Efficiency Comparison Between Standardized HFC and CO2 Transcritical Systems for Supermarket Applications[C]//Proceedings of the International Congress of Refrigeration (ICR), August 21-26, Prague, Czech Republic, 2011, ID: 357.

[19] Dokandari D.A., Hagh A.S., Mahmoudi S.M.S. Thermodynamic investigation and optimization of novel ejector-expansion CO2/NH3 cascade refrigeration cycles (novel CO2/NH3 cycle)[J]. International Journal of Refrigeration, 2014, 46, 26-36.

[20] Lawrence N., Elbel S. Review and analysis of the effect of ejector geometry on the performance of two-phase co2 ejectors[C]//11th IIR Gustav Lorentzen Conference on Natural Refrigerants, Hangzhou, China, 2014.

[21] Elbel S. Historical and present developments of ejector refrigeration systems with emphasis on transcritical carbon dioxide air-conditioning applications[J]. International Journal of Refrigeration, 2011, 34(7): 1545-1561.

[22] Banasiak K., Hafner A., Kriezi E.E. Development and performance mapping of a multiejector expansion work recovery pack for R744 vapour compression units[J]. International Journal of Refrigeration, 2015, 57, 265-276.

[23] Lucas C., Koehler J. Experimental investigation of the COP improvement of a refrigeration cycle by use of an ejector[J]. Int. J. Refrigeration , 2012, 35: 1595-1603.

[24] Xiong J., Eikevik T.M., Wang R.Z., et al. Experimental analysis of the influence of operating conditions on the performance (COP and ejector efficiency) of R744 heat pump with one-phase ejector[C]//11th IIR Gustav Lorentzen Conference on Natural Refrigerants (GL2014). Proceedings. Hangzhou, China, 2014.

[25] Gay N.H., 1931. Refrigerating system. U.S. Patent No. 1836318.

[26] Elbel S., Hrnjak P. Experimental validation of a prototype ejector designed to reduce throttling losses encountered in transcritical R744 system operation[J]. International Journal of Refrigeration, 2008, 31(3): 411–422.

[27] Lorentzen G, Pettersen J. New possibilities for non-CFC refrigeration[C]//International Symposium on Refrigeration, Energy and Environment, Trondheim, Norway, 1992:147-163.

[28] Lorentzen G. Revival of carbon dioxide as a refrigerant[J]. International Journal of Refrigeration, 1994, 17(5):292-301.

[29] Lorentzen G. The use of natural refrigerants: a complete solution to the CFC/HCFC predicament[J]. International Journal of Refrigeration, 1995, 18(3): 190-197.

[30] Hafner A., et al. High efficient 100 kwel r744 compressor[C]//The 10th IIR Gustav Lorentzen Conference on Natural Refrigerants, Delft, The Netherlands,

2012: 421-428.

[31] CompressorDB, Pack Calculation Pro: Version 3.02[CP]. IPU, 2016.

[32] Ge Y.T., Tassou S.A. Performance evaluation and optimal design of supermarket refrigeration systems with supermarket model "SuperSim". Part II: Model applications[J]. International journal of refrigeration, 2011, 34, 540-549.